이학박사 학위논문

Large-scale functional brain network for attentional regulation of encoding : Oscillatory interactions based on bipartite graph filtration

부호화에 대한 주의 조절의 뇌 기능적 신경망: 양분 그래프 필트레이션 기반의 오실레이션 관계 연구

2015년 2월

서울대학교 대학원

협동과정 인지과학 전공

함 자 랑

Large-scale functional brain network for attentional regulation of encoding : Oscillatory interactions based on bipartite graph filtration

지도교수 이 동 수

이 논문을 이학 박사 학위논문으로 제출함
2014년 12월

서울대학교 대학원
협동과정 인지과학 전공
함 자 랑

함자랑의 이학박사 학위논문을 인준함
2014년 12월

위 원 장 정 천 기 (인)

부위원장 이 동 수 (인)

위 원 김 청 택 (인)

위 원 강 은 주 (인)

위 원 강 혜 진 (인)

Large-scale functional brain network for attentional regulation of encoding : Oscillatory interactions based on bipartite graph filtration

Jarang Hahm

Interdisciplinary Program in Cognitive Science

The Graduate School

A Thesis Submitted to the Faculty of Interdisciplinary Program in Cognitive Science, in Partial Fulfillment of the Requirements for the Degree of Doctor of Philosophy in Science at the Seoul National University, Seoul, Korea

December 2014

Approved by thesis committee:

Chairman	**Chun Kee Chung**
Vice-Chairman	**Dong Soo Lee**
Member	**Cheongtag Kim**
Member	**Eunjoo Kang**
Member	**Hyejin Kang**

ABSTRACT

Large-scale functional brain network for attentional regulation of encoding : Oscillatory interactions based on bipartite graph filtration

Jarang Hahm
Interdisciplinary Program in Cognitive Science
The Graduate School
Seoul National University

To encode relevant information and also suppress irrelevant one is suggested to be important mechanism for efficient memory functioning in the brain. The neural correlates of such memory regulation has been suggested as intra-regional interactions between alpha and gamma cross-frequency power. The current study expanded the cross-frequency interactions into a large-scale regional network for memory regulation. I analyzed the data wherein twenty-three healthy subjects were instructed to remember (“Remember”) or not to remember (“No-Remember”) the following picture item by a cue during

magnetoencephalography (MEG) recording. In this setting, network was modeled by correlation between regions (i.e. nodes) for alpha power during cue presentation and regions for gamma power during item presentation, yielding a bipartite graph. Then, graph filtration method was applied to bipartite graph, wherein the changes of connected components between two sets of nodes were quantified into two invariant measures: a barcode and single linkage distance. This procedure was called bipartite graph filtration in this study. As a result, as for the global connectivity reflected by the barcode, task condition was significantly different for gamma power during item presentation. In addition, subjects with steeper barcode in “Remember” than in “No-Remember” condition showed higher compliance to task instruction. Also, for “Remember” condition, subjects with fast merging pattern in alpha power during cue presentation than the pattern in gamma power during item presentation showed better memory performance. These findings suggested that encoding regulation is achieved by large-scale regional interactions, and the property of cognitive function is captured by pattern of network. As for the local connectivity reflected by single

linkage distance, the connectivity between the left dorsolateral superior frontal gyrus for alpha power and the left insula for gamma power was significantly closer in “Remember” than in “No-Remember” condition. The superior frontal gyrus was included in dorsal attention network, suggesting dorsal attentional regulation of later long-term memory in the insular cortex. In conclusion, encoding regulation was investigated by large-scale brain interactions using bipartite graph filtration, showing the method allows to examine the time-lagged interactions between different frequency powers in an MEG network study for the first time.

Keywords: functional brain network, alpha oscillation, gamma oscillation, magnetoencephalography (MEG), memory, attention, graph filtration

***Student Number*:** 2012-30033

CONTENTS

List of Figures

List of Tables

1. Introduction

1.1. The control mechanism for efficient memory function

It has been suggested that the brain not only need to encode relevant information, but also need to inhibit irrelevant one for an efficient memory functioning (Anderson & Green 2001, Anderson & Levy 2009, Van Hooff et al 2009). To study on the mechanism underpinning such voluntary memory control, several task paradigms has been employed such as “Think/No-Think” or “To-be-remembered/Not-to-be-remembered” paradigm.

The Think/No-Think paradigm instructs subjects to repeatedly either recall or suppress previously seen materials in terms of memory retrieval. The documented findings demonstrated that the Think/No-Think paradigm resulted in enhancing later memory for recalled items, and also later forgetting for suppressed items (Anderson & Green 2001, Anderson et al 2004, Depue et al 2007). Further, the voluntary control of retrieval have shown to be enhanced by prior information on whether suppress or recall the upcoming items when compared to the absence of

the information (Hanslmayr et al 2010). This demonstrated that the voluntary control of irrelevant memories benefit from the preparatory phase, suggesting that brain activation prior to stimulus exert efficient regulation for later memory in terms of retrieval.

1.2. Brain oscillation in encoding regulation

The neural mechanism underlying memory regulation has been investigated using various imaging modalities (Anderson & Levy 2009, Anderson et al 2004, Depue et al 2007, Freunberger et al 2009, Hanslmayr et al 2009). Among a variety of measure of brain activity, brain oscillation has been suggested to be appropriate for study on the physiological basis of cognitive function (Buzsaki & Watson 2012, Thut et al 2012). Neural oscillations refer to periodic fluctuations of activity in neuronal population, which span a variety of frequencies and location in cerebral cortex. (Buzsaki & Watson 2012, Schnitzler & Gross 2005). The oscillation has been suggested to represent neuronal communication in that the generation of oscillations has been shown to depend on cellular pacemaker mechanism and neuronal network

properties (Bennett & Zukin 2004).

One study have examined brain oscillation related to control mechanism of memory in terms of working memory encoding using ‘To-be-remembered/Not-to-be-remembered’ paradigm (Freunberger et al 2009). In the task, a cue was presented prior to the stimuli, informing the subjects whether remember (‘To-be-remembered’) or do not remember the next stimuli (‘Not-to-be-remembered’) while the brain activity was measured using electroencephalography (EEG). They found that the ‘Not-to-be-remembered’ condition showed increased alpha oscillatory power in posterior regions prior to stimulus presentation compared to ‘To-be-remembered’ condition. The result suggested that pre-stimulus alpha power reflect top-down control of later encoding.

1.2.1. The previous study of encoding regulation in terms of long-term memory

The brain oscillation engaged in encoding regulation have also scrutinized in terms of long-term memory using MEG (Park et al 2014)

which I collaborated on. In fact, the current study proceeded based on the previous study by handling with the same data set. Thus, in this section I summarized the main findings of the previous study before describing the present study.

The previous study exploited a long-term memory paradigm consisting of encoding and recognition session. In the encoding session, a trial consisted of three phases: cue, item, and inter-trial interval. Those three phases were presented in turn. The cue phase presented a fixation cross colored in either yellow or blue (Figure 1A). According to the color of fixation cross, subjects was instructed to remember ("Remember" condition) or not to remember the upcoming item ("No-Remember" condition).

The time-frequency analysis found alpha oscillatory power, especially around 10 Hz, was stronger in "No-Remember" than in "Remember" condition during cue interval in posterior regions (Figure 1B). In addition, the alpha power showed a positive relationship with task performance. It supported that alpha oscillatory activity in dorsal attention network exerts top-down control for the forthcoming

encoding.

Further, when the alpha oscillation plays control mechanism over encoding, the main interest is how the control function by alpha oscillatory power modulates encoding. To answer this question, gamma oscillatory power was analyzed. Gamma band oscillation, which range over 30 Hz, has been demonstrated to engage in active memory processing such as encoding and maintenance (Jensen et al 2007, Jerbi et al 2009, Park et al 2011, Pesaran et al 2002). Thus investigation of the relationship between alpha oscillation during cue and gamma oscillatory power in item presentation might be helpful to elucidate the mechanism of encoding regulation. For the gamma band, stronger power was found around 80 Hz during item presentation in “Remember” condition compared to “No-Remember” condition (Figure 1B), suggesting active encoding processing during item interval in “Remember” condition.

In the end, the cross-frequency power interaction was examined between changes of power between alpha (10 Hz) oscillation during cue presentation and gamma (80 Hz) band power in item

presentation by focusing on the bilateral precuneus. It showed that those who showed greater alpha power during cue presentation in “No-Remember” than in “Remember” condition exhibited stronger gamma power during item presentation in “Remember” than in “No-Remember” condition. Taken together, the previous study concluded that pre-stimulus top-down control gates information to long-term memory by neural synchrony between pre-stimulus alpha and later gamma oscillatory power in the posterior region.

A Long-term memory paradigm : Encoding session

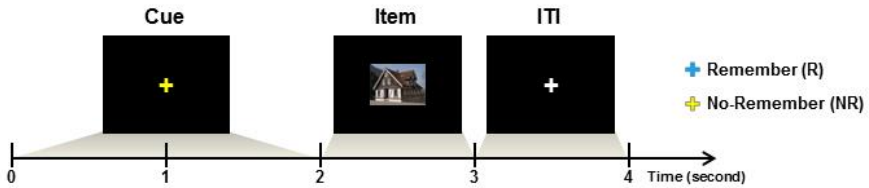

B Time-Frequency Representation

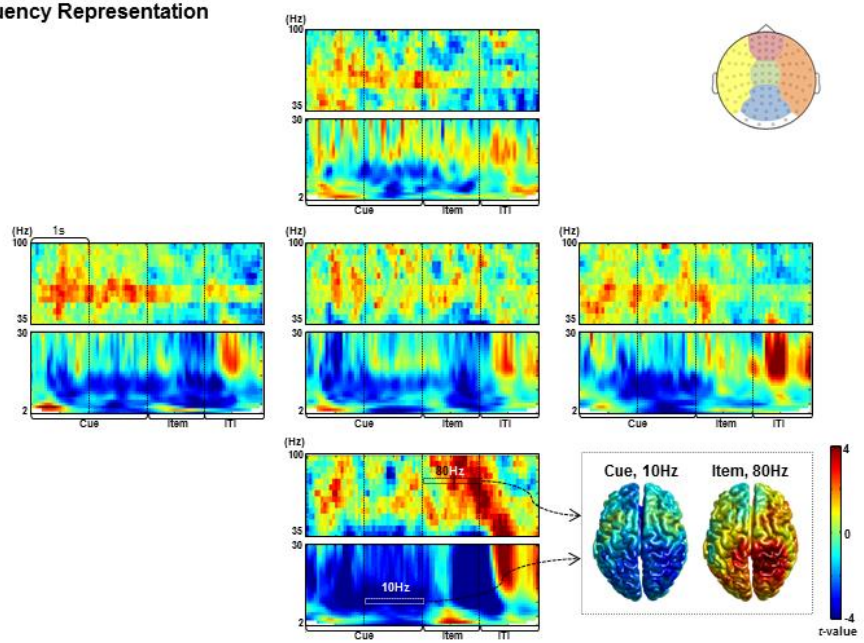

Figure 1. Task Paradigm and Time-Frequency Representation of the previous findings. (A) The encoding session of a cued long-term memory paradigm. In the encoding session, a picture item was presented to participants after cue exhibition. A color of cue indicated a type of task, which is to remember ("Remember") or not to remember ("No-Remember") the upcoming item. The participants were instructed to perform as the cue indicated. After the end of the encoding session, subjects' memory performance was tested. (B) Time-frequency representation during task. The *t*-statistics between two task conditions ("Remember" vs "No-Remember") were shown. The sensors were grouped into five regions shown by different colors on topoplot in the bottom right corner. Within each region, power spectrum of the sensors was average to be tested. The range of frequency was selected based on $p < 0.05$: 10 Hz during cue presentation (1-2 s) and 80 Hz during item presentation (2-3 s), which was stronger in posterior region.

1.2.2. The proposal from the previous study

The previous study focused only on within-regional neural synchrony, especially in the precuneus since it exhibited stronger difference between conditions for each alpha and gamma power. Considering the precuneus belongs to the dorsal attention network, they suggested that dorsal attention network gates later encoding processing. The documented findings on the relationship between attention and memory demonstrated that both dorsal and ventral attentional networks are involved in memory function (Burianova et al 2012, Chun & Turk-Browne 2007, Ciaramelli et al 2008, Gazzaley 2011).

Also, in terms of alpha oscillatory power, its role of functional inhibition has been found mainly in parietal and occipital regions (Freunberger et al 2009, Johnson et al 2010, Meeuwissen et al 2010), however several studies has also found other regions such as motor (Haegens et al 2010, Pfurtscheller & Lopes da Silva 1999), sensory (Ai & Ro 2014) and frontal regions (Maclin et al 2011). These findings suggested that distributed regions are involved in functional inhibition by alpha oscillation (Haegens et al 2010).

In fact, the power spectrum of the previous long-term memory study showed alpha oscillatory power and gamma band power along large-scale spatial dimension (Figure 1B). Thus, the neural correlates for encoding control reflected by interaction between alpha oscillation and gamma band activities needs to be examined not only within single region, but also between regions (Figure 2A).

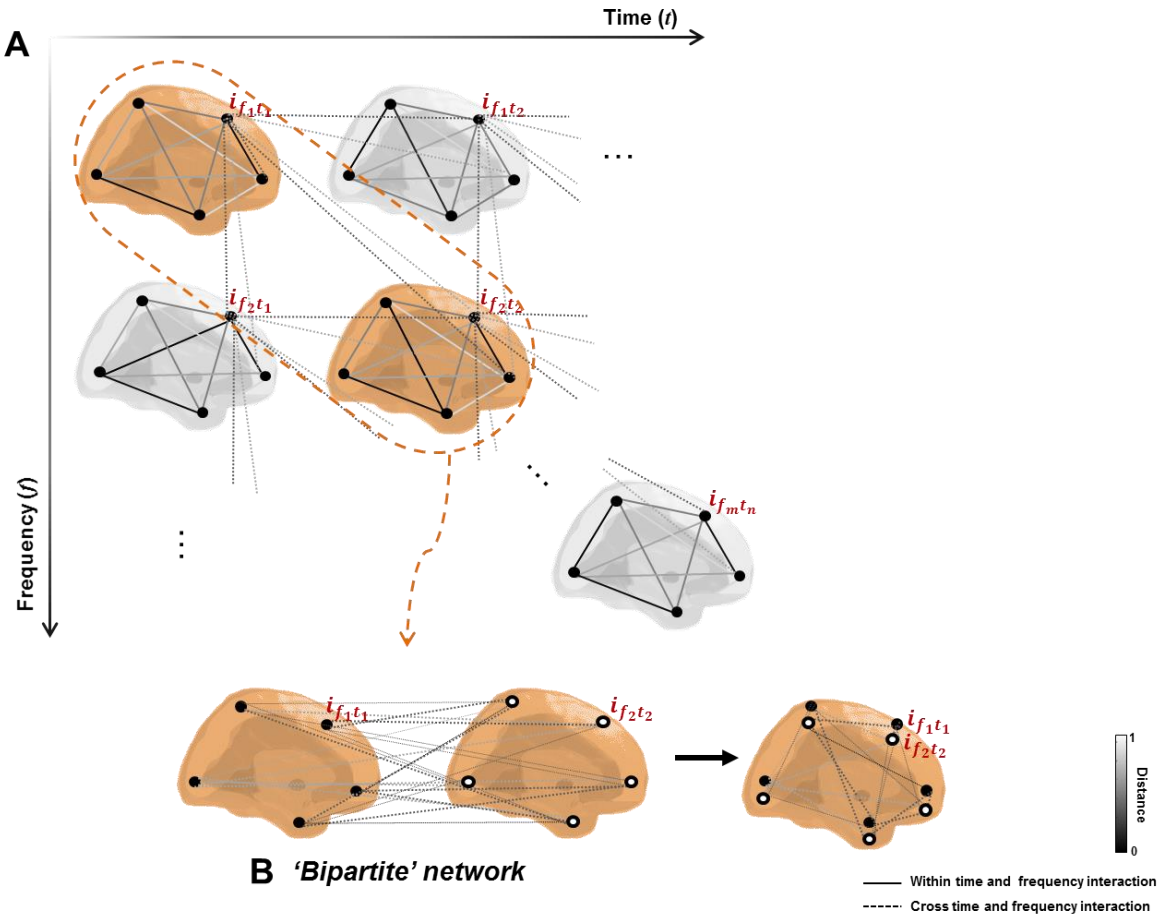
A
Time (t)
Frequency (f)
$i_{f_1t_1}$
$i_{f_1t_2}$
$i_{f_2t_1}$
$i_{f_2t_2}$
$i_{f_mt_n}$
B 'Bipartite' network
Distance
1
0
Within time and frequency interaction
Cross time and frequency interaction

Figure 2. Schematic representation of functional network organization in the brain. A) Cognitive functions is suggested to be achieved through an active network in a spatio-temporo-spectral dimension by modulating the strength of functional connections among distributed regions in the brain. One region is assumed to be fully linked with the other regions directly (i.e., via anatomical connection) or indirectly (i.e., via functional connectivity defined by statistical dependency between two regions), while the figure displayed a few interactions as an example. B) Of multiple dimensions, the present study focused on interactions between different time and frequency band, which is colored in orange. Those different set of time and frequency band consisted of separable nodes of network, and edges were estimated only between two sets of nodes. This kind of network is called bipartite network, which is modeled for investigating encoding regulation in the present study.

1.3. The distributed network organization for cognitive function

In fact, cognitive processing in the brain involves in interactions among distributed assembles of neurons (Bressler 1995, McIntosh 2000, Varela et al 2001). It has been supported by electrophysiological study showing synchronization between distant cortical regions. For example, a study of local field potential (LFP) on monkey brain showed coherence between visual and motor area when making motor responses (Bressler et al 1993). And this large-scale interactions also found in human brain using invasive tools such as EEG and MEG, suggesting that information processing is suggested to be performed by synchronizing oscillatory activities across spatially distributed neuronal populations (Destexhe et al 1999, Fries et al 2001, Gevins et al 1987, Palva & Palva 2012, Siegel et al 2012, Steriade 1997).

If the large-scale network underlie cognitive function, then how dose cognition emerge in terms of large scale cortical network? McIntosh (2000) suggested the idea of “neural context” wherein the interactions among regions are key features of ongoing functional

properties rather than the size of neural activity in single region. For example, the well-known dorsal stream can be explained by stronger inter-regional connectivity between occipital and inferior temporal region in the object recognition task, while the ventral stream showed stronger connectivity between occipital and parietal region, and between parietal and frontal region in spatial vision task (McIntosh & Gonzalez-Lima 1994). Likewise, multiple cognitive functions are suggested to be emerged by rapid reconfigurations of inter-regional functional connectivity according to ongoing functional state (Bressler & McIntosh 2007, Bressler & Tognoli 2006, Lenartowicz & McIntosh 2005, McIntosh 1999). Thus, the examination of functional connectivity patterns in a large scale network can shed light on the characteristics of ongoing functional state.

1.4. Large-scale brain network based on bipartite graph filtration

The functional connectivity can be modeled as a network or graph which consists of nodes and edges connecting nodes. For the current study, the network consisted of two sets of nodes: regions of

alpha power during cue presentation (‘cue alpha’) and regions of gamma power during item presentation (‘item gamma’). And the interactions were estimated only between the node sets. This type of graph is called bipartite network (Figure 2B), which is expected to allow to examine time-lagged and cross-frequency interaction in a form of network.

For the network analysis, most brain network study frequently transformed the network into a binary adjacency matrix which indicated the absence or presence of edges between nodes. Then, quantitative graph theoretical measures were calculated such as clustering coefficient or characteristic path length, then the node with the highest or lowest value of graph metric was found (Bullmore & Sporns 2009, Bullmore & Bassett 2011, Sporns 2011).

Before computing graph theoretical metrics, most of network studies apply a threshold on the estimated edge weight in order to obtain a binary graph where the edge weight above a given threshold level is counted otherwise ignored. Thus thresholding a graph defines the number of edges in graph. Considering the graph theoretical

measures depend on the number of edges, the graph measure can be changed as a function of a threshold level (Lee et al 2011a). However there is no gold standard on definition of the proper threshold level. Also a thresholded network usually contains the stronger edges while discarding the weaker ones although the weak edges has been suggested to be relevant to cognitive functions such as attention and memory, also to pathology (Bassett et al 2012). Thus the network thresholding can lead to information loss. In these reasons, network thresholding is one of the crucial issue in network construction (Wig et al 2011).

To circumventing the issue of network thresholding, Lee and colleagues proposed a novel threshold-free approach for large-scale brain network using graph filtration (Lee et al 2011a, Lee et al 2011b). In this method, any nodes connected with the distance less than a certain threshold make a connected component. At the beginning, the threshold is zero, so that every single nodes are regarded as a connected component. As the criterion grows from zero to one, the size of connected component (i.e., the number of nodes belonging to the

connected component) gets bigger by merging with other connected components. Finally all the components are converged to form the largest connected component by belonging to the single connected component. This procedure is called graph filtration and the threshold of distance is called filtration value. By covering all filtration values, the method does not need network thresholding. Also it provides network invariants such as a barcode and dendrogram (Lee et al 2011b), where the barcode reveal multi-scale functional connectivity pattern through filtration. Considering the connectivity patterns may represent the ongoing functional state, the barcode is useful to investigate functional network engaged in memory regulation.

Taken together, I applied graph filtration method to bipartite graph, yielding bipartite graph filtration. The method will enable to see changes in multi-scale connectivity between different time and frequency band in the MEG network analysis for the first time.

1.5. The aim and hypothesis of the present study

The present study aimed to investigate neural correlates of

encoding regulation by analyzing large-scale brain cross-frequency interactions between ‘cue alpha’ and ‘item gamma’ power based on bipartite graph filtration. Then invariant features of the network was extracted and compared between task conditions to examine how pre-stimulus brain activity influence on later encoding process in terms of connectivity. Then I expected to find that, first, global network changes reflected by a barcode is distinctive between “Remember” and “No-Remember” condition. And, second, the local inter-regional relationships show task condition difference.

2. **Materials and Methods**

I employed the previously reported data (Park et al 2014). The procedure from preprocessing to source localization was the same with our previous research. However, the current study went a step further to investigate a large-scale network using the graph filtration method. In this section, I briefly described procedure from preprocessing to source localization (See Park et al (2014) for more details), while network analysis in detail.

2.1. Participants

Twenty-three healthy subject data (11 males and 12 females, mean age of 24.8 ± 3.1) were included for analysis. All of the participants were right-handed and had normal or corrected-to-normal vision. None of the participants had any history of developmental, psychological, or neurological disorders. This study was approved by the Institutional Review Board (IRB) at Seoul National University Hospital (IRB No.

C-1007-156-325). All the participants completed the written informed consent before the experiment.

2.2. Experimental paradigm and procedure

A cued long-term memory paradigm was employed. In the encoding session, a trial consisted of three phases: cue, item, and inter-trial interval (ITI). After presentation of cue for 2 s, item was presented for 1 s, followed by ITI for 1 s (Figure 1A). Subjects were instructed either to remember ("Remember" condition) or not to remember ("No-Remember" condition) the upcoming picture item depending on a color (i.e., yellow or blue) of the prior fixation cross. The item were real-life photographs of landscapes or buildings. The visual angle of items was 8° horizontally (334 x 250 pixels) and projected to a screen by using STIM2^{TM} software (Compumedics Neuroscan, Charlotte, NC). Each condition consisted of two hundreds trials. In addition, twenty trials were included, which contained a perceptual decision phase after item presentation wherein the subject responded whether previously

displayed item was a building or landscape by pressing a button in order to ensure that the subject attended the item during item presentation. Finally each condition had two hundred and twenty trials. After the encoding session, the recognition session started after a brief interference task using simple arithmetic calculation. The total forty hundred and forty items were randomly intermixed with two hundreds of new items (“New”) as memory foils. The participants were given three buttons, i.e., “old”, “don’t know”, and “new”, and responded by pressing a button while each item was presented on the screen for four seconds.

2.3. Behavioral measurement

All the trials of recognition session were categorized by the response during the recognition session, as follows. The old and new responses for the trials of “Remember” condition (R) were tagged as R-hits and R-misses, respectively. And those for the “No-Remember” condition (NR) were tagged as NR-hits and NR-misses, while those for the “New” condition as false alarms and correct rejections. To quantify the

degree to which a subject followed the instruction depending on a cue sign, task compliance was defined by calculating the standard *d*-prime of R-hits minus NR-hits. And also memory performance was defined by the standard *d*-prime of R-hits minus false alarms.

2.4. MEG measurement

Brain electromagnetic activities were measured during encoding session using a whole-head MEG Neuromag (VectorViewTM, Elekta Neuromag Oy, Helsinki, Finland) acquisition system installed at the MEG center of Seoul National University Hospital. The vertical and horizontal electrooculogram (EOG) and electrocardiogram (ECG) was also recorded to remove eye movements and cardiac artifacts. All subjects entered the electromagnetically shielded and sound attenuated room after being attached head position indicator (HPI) coils sparsely on the head, and identified anatomical landmarks such as nasion and bilateral preauricular points by 3D digitizer (FASTRAKTM, Polhemus, Colchester, VT). Then HPI coils in the MEG machine registered the subject's head position, allowing the reconstructed sources of MEG

signal to be overlaid on structural MR images with high precision. Before data analysis, a Maxwell filter (Signal Space Separation) was adopted to reduce the confounding possible influence of biological and environmental noises (Taulu & Simola 2006, Taulu et al 2005).

2.5. Structural MR image acquisition

For the source localization of MEG signal, T1-weighed MR images were acquired by gradient echo pulse sequence (repetition time 1.67 s, echo time 1 ms, and flip angle 9°) at 3 Tesla using a Siemens Trio Tim scanner (Siemens, Erlangen, Germany), yielding 208 sagittal slices with 1.0 x 0.98 x 0.98 mm^3 voxel size.

2.6. Data analysis

The data were analyzed using the Fieldtrip open source software package (the Donders Institute for Brain, Cognition and Behaviour, Centre for Cognitive Neuroimaging,Nijmegen, The Netherlands, http://fieldtrip.fcdonders.nl) (Oostenveld et al 2011) and in-house

scripts in Matlab (2013a, MathWorks, Natick, MA, USA). Before the analysis, the data were downsampled at 600 Hz after applying a low-pass filter at 200 Hz due to computational burden. Trials tainted with SQUID jump and muscle artifacts were visually selected to be rejected, and then EOG and ECG artifacts were removed using independent component analysis (ICA).

2.7. Spectral analysis

After artifact removal, time-frequency representations of power were calculated in two distinct frequency ranges. For lower frequencies (1-32 Hz), spectral power were computed based on a sliding time window shifted in steps of 50 ms covering the whole trial length of 4s. The length of the sliding time window was adapted to the frequency containing four cycles (i.e., $\Delta T = 4/f$, e.g. 400 ms for 10 Hz). Prior to the Fourier transformation, the data segments of the sliding time windows were tapered with a Hanning window, resulting in adaptive spectral smoothing of $\Delta f \sim 1/\Delta T$. For high frequency ranges (20-200 Hz), a time window of 200 ms length was applied with a multitaper

approach involving three orthogonal Slepian tapers resulting in a spectral smoothing of ~10 Hz (Percival & Walden 1993).

The spectral power was normalized by mean of two conditions for each sensor, frequency, condition, and subject. To observe spatial power changes between conditions, the sensors were grouped into five areas (i.e., front, vertex, bottom, left, and right) and the power were averaged across sensors within the area. The *t*-value of condition difference was displayed in Figure 1B.

2.8. Source analysis

To reconstruct sources in frequency domain, the sources of the oscillatory activities were identified using a beamforming approach based on an adaptive spatial filter (Dynamic Imaging of Coherent Sources, DICS) (Gross et al 2001). First, the two distinct frequency and time window were research of interests based on the previous report (Park et al 2014): 10 Hz during cue presentation (1-2 s, latency 1 s; ‘cue alpha’ as described above) and 80 Hz during item presentation (2-3 s, latency 1 s; ‘item gamma’ as described above).

For Fourier transformation, multitaper method was used to compute spectrum for the entire segmented data length (1 s). For 10 Hz, a Hanning taper was applied, leading to 3 Hz smoothing for a 500 ms window, while three Slepian tapers for the gamma frequency (80 Hz) resulting in a 10 Hz spectral smoothing. The cross-spectral density matrices were calculated for each Fourier transformed data for each time window, frequency, condition, and subject.

From each individual's MRI, realistically shaped single-shell descriptions of the brains were constructed. Each subject's brain volume was discretized into a grid with a 0.8 cm resolution and spatially normalized to the template MNI brain (International Consortium for Brain Mapping, Montreal Neurological Institute, Canada) by using SPM8 (http://www.fil.ion.ucl.ac.uk/spm).

The lead field was computed at every grid point. A spatial filter was formed for each grid point using the cross-spectral density matrices for the frequency of interest and the lead fields. In the end, the spatial distribution of oscillatory power was computed for each condition by applying the common filter for both conditions. The source power

spectrum was normalized by mean of each source spectral power and source of ITI phase (latency 1 s, 3-4 s; 'ITI alpha' and 'ITI gamma') at single trial level. For example, 'cue alpha' source was normalized by mean of 'cue alpha' source and 'ITI alpha' source for each trial, subject and condition. The normalized source power for each cue alpha and item gamma were displayed in Supplementary figure 1.

2.9. Network analysis

2.9.1. Network construction

Network consists of a set of nodes and edges linking nodes. First of all, nodes were defined by region of interests (ROIs) using the Automated Anatomical Labeling (AAL) atlas (Tzourio-Mazoyer et al 2002) consisting of thirty-eight regions for each hemisphere after excluding subcortical and cerebellar areas (Table 1). AAL atlas space was interpolated into an individual source grid space, and then source power values were averaged within each ROI (Figure 3A), yielding trials-by-ROIs power matrices for each cue alpha and item gamma per subject and condition. Then, edges were given by estimating Pearson's

correlation coefficient between trials-by-ROIs power matrices of ‘cue alpha’ and ‘item gamma’ for each subject and condition. In fact the number of trials between two task conditions was different for each subject due to trial rejection for artifact removal. Considering correlation coefficient can be affected by the number of observations (i.e., trials) (Gross et al 2013), the number of trials was adjusted to the minimum number of trials between two conditions by performing random selection of trials for each subject. Then Pearson’s correlation coefficient was estimated between the two power matrices (Figure 3B). After computing correlation coefficients over trials, a ROIs-by-ROIs correlation matrix was made for each subject and condition. Each row and column of correlation matrix indicated ROIs from each ‘cue alpha’ and ‘item gamma’ nodes. Then, correlation coefficients were estimated. Considering the findings of our previous study, the decreased alpha power during cue presentation represented the opening of a gate to memory system, so that it was related to increased gamma band power during item presentation. Whereas, increased alpha power indicated blocking later encoding process, which was related to decreased

gamma power during item interval. Likewise, the pre-stimulus regulation over later encoding process is suggested to be operated by negative relationship between alpha oscillatory power and gamma band activity for each condition. Thus, in the current study, only negative correlation coefficients were taken into account for analysis.

Table 1. The list of region of interests (ROIs) used for network analysis. Total 38 regions for each hemisphere were selected except for subcortical and cerebellar regions.

No.	Regional category	Anatomical description	Abbreviation
1	Frontal	Olfactory cortex	OFC
2		Gyrus rectus	Rectus
3		Inferior frontal gyrus, orbital part	IFG.orb
4		Inferior frontal gyrus, opercular part	IFG.oper
5		Inferior frontal gyrus, triangular part	IFG.tri
6		Middle frontal gyrus, orbital part	MFG.orb
7		Middle frontal gyrus	MFG
8		Superior frontal gyrus, orbital part	SFG.orb
9		Superior frontal gyrus, medial orbital	MFG.orb
10		Superior frontal gyrus, medial	SFG.med
11		Superior frontal gyrus, dorsolateral	SFG.dl
12		Paracentral lobule	Paracentral
13		Supplementary motor area	SMA
14		Precentral gyrus	Precentral
15		Rolandic operculum	Rolandic.oper
16	Limbic	Anterior cingulate and paracingulate gyri	Cing.ant
17		Median cingulate and paracingulate gyri	Cing.mid
18		Posterior cingulate gyrus	Cing.post
19	Parietal	Postcentral gyrus	Postcentral
20		Superior parietal gyrus	SPC
21		Precuneus	PreCu
22		Inferior parietal, but supramarginal and angular gyri	IPC
23		Supramarginal gyrus	SMG
24		Angular gyrus	AG
25	Temporal	Superior temporal gyrus	STG
26		Heschl gyrus	Heschl
27		Middle temporal gyrus	MTG
28		Inferior temporal gyrus	ITG
29		Temporal pole: superior temporal gyrus	TP.STG
30		Temporal pole: middle temporal gyrus	TP.MTG
31		Insula	INS
32	Occipital	Fusiform gyrus	Fusi
33		Inferior occipital gyrus	IOC
34		Middle occipital gyrus	MOC
35		Superior occipital gyrus	SOC
36		Calcarine fissure and surrounding cortex	Calcarine
37		Cuneus	Cu
38		Lingual gyrus	Ling

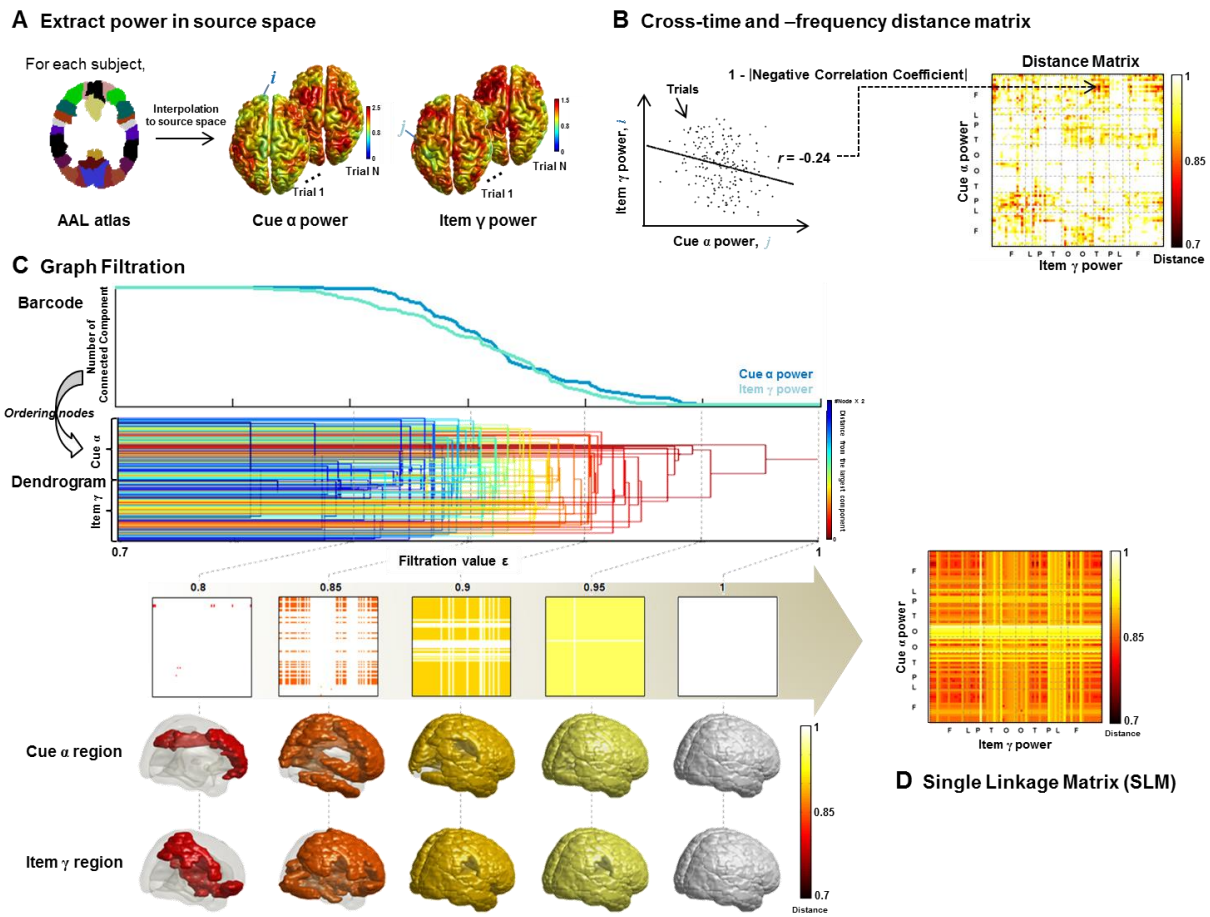
A Extract power in source space
For each subject,
Interpolation to source space
AAL atlas
Cue α power
Item γ power
Trial 1
Trial N
B Cross-time and –frequency distance matrix
1 - |Negative Correlation Coefficient|
Trials
r = -0.24
Item γ power, i
Cue α power, j
Distance Matrix
Cue α power
Item γ power
Distance
C Graph Filtration
Barcode
Number of Connected Component
Cue α power
Item γ power
Ordering nodes
Dendrogram
Cue α
Item γ
Filtration value ε
0.7
1
0.8
0.85
0.9
0.95
Cue α region
Item γ region
D Single Linkage Matrix (SLM)

Figure 3. Pipeline of the network analysis using graph filtration method. For each subject and condition, we performed network analysis using graph filtration. To illustrate the procedure, "Remember" condition of one subject was displayed. A) Node is defined by AAL atlas regions after excluding subcortical and cerebellar regions. AAL atlas was interpolated into the source grid space, and then source power was extracted and averaged within each region. B) Power-to-power Pearson's correlation coefficient was calculated between alpha oscillatory power during cue ('cue α power') and gamma band activity during item presentation ('item γ power'). And negative correlation coefficient was converted into distance by 1 - absolute of negative correlation coefficient. C) By applying graph filtration method, a barcode and single linkage matrix was calculated.

2.9.2. Graph filtration

I first defined a distance function $d(x,y)$ by 1- absolute of negative correlation coefficients, where *x* is a node of 'cue alpha' and *y* is a node of 'item gamma'. As a distance, ε, goes from 0 to 1, I connected any node pairs when their distance is less than ε (i.e., $d(x,y) \leq \varepsilon$). Thus it can form a nested sequence of the thresholded or unweighted networks over distances, which is called graph filtration. The ε is a filtration value. Among a variety of topological features, the present study observed the number of a connected component in network as a topological feature, and visualized it by plotting the birth and the death intervals of every connected component in a range of the filtration value. The obtained network was a bipartite network whose nodes are divided into two disjoint sets (i.e., 'cue alpha' and 'item gamma'), so that finally the barcode was separated for each node set (Figure 3C). The whole graph filtration procedure was simplified to display by using an example data for better understanding of it (Supplementary Figure 2).

For the bipartite graph, there were different sets of nodes, 'cue

alpha' and 'item gamma.' For each set of nodes, a barcode can be re-computed (Supplementary figure 3). By dividing into two barcodes, the interactions between two sets of nodes can be elucidated by comparing two barcodes within each condition. For example, if one node of one node set was connected to one node of the other set (1 : 1), the two separated barcodes were the same in terms of the number of connected component over filtration values or the slope of barcode. On the other hand, if several nodes of one set were connected to single node of the other set (m : n, where m > n), the barcode of the former nodes sets were steeper than that of the latter one. Likewise, comparison between separated barcodes provided information on configuration of large-scale connectivity between node sets.

Note that although the barcode is divided into two separated barcodes for each node set, i.e., 'cue alpha' and 'item gamma', the property of bipartite graph was preserved for each separated barcode since barcode separation was based on the initial one which was defined by the connectivity only between sets of nodes, not connectivity within each set of nodes. Also note that after barcode

separation, nodes belonging to the same connected component within one network can be interpreted to interact one another as suggested by Lee et al (2012) wherein the regions in the same component share the information through diffusion even though I did not directly model the edges between the same set of nodes.

In fact, the barcode shows global topological changes by ignoring geometric information of nodes. However, for a brain network, it is important to know nodal contributions to their topological changes. To investigate local changes, nodes of the barcode were sorted along geometric information, yielding a single linkage dendrogram (Lee et al 2012). To compare the single linkage dendrogram between conditions, it was transformed into a matrix form, generating single linkage matrix (SLM) (Figure 3D).

In sum, through filtration, the changes of the number of connected component was counted and quantified as a barcode and SLM. A barcode can show global network changes while an SLM can exhibit local network changes for each task condition.

2.10. Statistical analysis

First, to find the difference in barcodes between two task conditions, I computed the difference of the number of connected component between two barcodes at every filtration value. The maximum amount of difference of the barcode was found between task conditions for each ‘cue alpha’ and ‘item gamma’ (from now on, they were called task phase for simplification), and between task phases for each condition. To reveal which side of the barcode is greater than the other, the plus or minus sign of the maximum difference was preserved. Then, the *t*-statistic of maximum differences across subjects (‘observed statistic’) was tested using a non-parametric method. The null hypothesis was that barcodes between task conditions (or between task phases) are not different, so that the barcodes of two conditions (or those of two task phases) was exchangeable to make a null distribution. It was done for almost half of the subjects who were selected randomly. And then the maximum amount of difference between barcodes was calculated while its plus or minus sign was preserved. A *t*-statistic for differences across subjects was calculated (‘randomized statistic’). This

procedure was iterated 10,000 times to yield a null distribution. Finally the observed *t*-statistic was tested at $p < 0.05$ based on the null distribution.

Second, the significance of edges in the SLM was tested based on the non-parametric method (Figure 4) which was the same as the test for the barcode described above. The significant edge was found at $p < 0.0005$. In fact, to find significant edges I needed to correct for the multiple comparisons to control false positive rate. However, the correction left no significant edges. In fact, the correction seemed to be quite conservative to produce false negatives. Rather I focused on the edges satisfying the following criteria for interpretation: i) survival at $p < 0.0005$ without multiple comparison correction, and ii) the edges showing either significant correlation ($p < 0.05$) with behavioral performance or showing significant functional connectivity ($p < 0.05$) when using the method of the previous study.

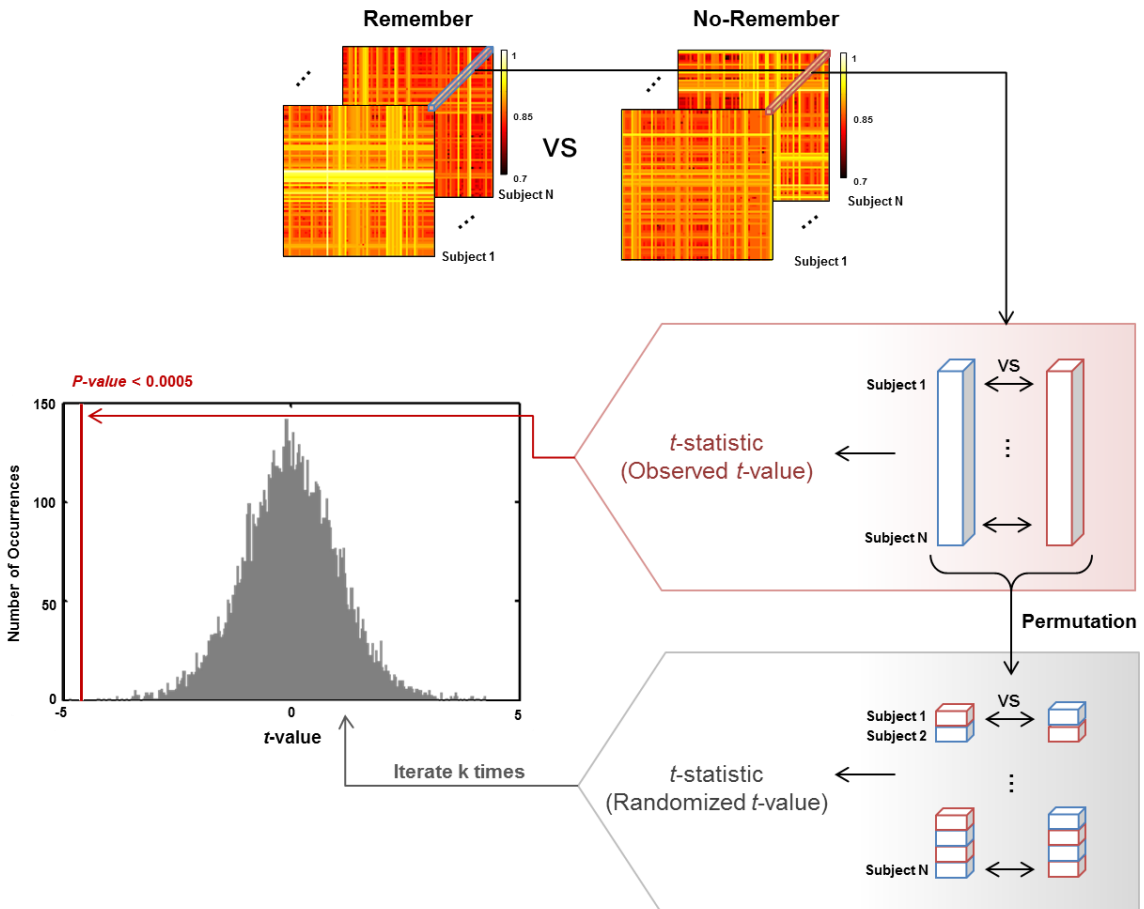
Remember
No-Remember
VS
1
0.85
0.7
Subject N
Subject 1
P-value < 0.0005
Number of Occurrences
150
100
50
0
-5
0
5
t-value
t-statistic
(Observed t-value)
Permutation
Iterate k times
t-statistic
(Randomized t-value)
Subject 2

Figure 4. Significance testing on single linkage distance using a permutation method. To test significance at every entry of single linkage matrix (SLM), we calculated a paired *t*-statistic and tested the significance using a non-parametric method. A null distribution was formed by switching the condition of SLMs with its subject pair preserved and calculated paired *t* -statistic, yielding a randomized *t* -value at every SLM entry. Then this procedure was repeated 10,000 times (k = 10,000). Then, *p*-value was calculated based on the null distribution and find significance at $p < 0.0005$.

3. Results

3.1. Behavioral performance

For the recognition rate, the ratio of R-hits (56.7 % ± 3.2 %) were significantly greater than that of NR-hits (33. 3% ± 2.2 %) ($t_{(22)}$ = 12.3, p < 0.001). This findings indicated that the subjects followed the instruction by remembering “Remember” item while ignoring the “No-Remember” item. Also, each the ratio of R-hits and NR-hits were bigger than the ratio of false alarm rate (24.2 % ± 2.0 %) significantly ($t_{(22)}$ = 14.5, p < 0.001 and $t_{(22)}$ = 9.0, p < 0.001, respectively). This showed that guessing rate was lower. See Park et al (2014) for more details.

3.2. Global network property measured by barcode

The network feature was extracted based on bipartite graph filtration, yielding two different forms: barcode and SLM. As for the barcode reflecting global network changes, each barcode of ‘cue alpha’

and ‘item gamma’ was compared between conditions. To see the group pattern of barcode for each task phase, the mean of barcodes across subjects was plotted, showing that the regions for “Remember” condition was merged the largest component faster than the nodes for “No-Remember” condition for each task phase (Figure 5A). After significance testing, the barcodes of the ‘cue alpha’ did not show the significant difference between conditions ($t_{(22)}$ = -1.72, p = 0.11, permutation) (Figure 5A, small figure in the left-sided plot), but the barcode of the ‘item gamma’ showed significant difference between conditions ($t_{(22)}$ = -2.71, p = 0.02, permutation) (Figure 5A, Small figure in the right-sided plot).

And then, to examine whether barcode differences between conditions explain the variance of task performance, correlation coefficient was calculated between task compliance (i.e., R-Hits vs. NR-Hits) and the maximum amount of differences in barcode between conditions for each ‘cue alpha’ and ’item gamma.’ For the ‘cue alpha’, did not showed significant correlation (r = -0.39, p = 0.07) (Figure 5B, Left), while the ‘item gamma’ showed significant correlation between

the difference of barcode between conditions and task compliance (r = -0.50, p = 0.02) (Figure 5B, Right). This result indicated that individuals with fast merging among regions in “Remember” than “No-Remember” condition exhibited better compliance. This finding was visualized in form of barcode in Figure 5C. Yellowish color reflected an individual who showed faster merging of regions in “Remember” than “No-Remember” condition, and showed better performance in task compliance. Considering merging patterns among regions represented by the barcode indicated the integration of large-scale brain regions, the findings demonstrated that the large-scale integration is distinctive between task conditions and is predictive of task compliance.

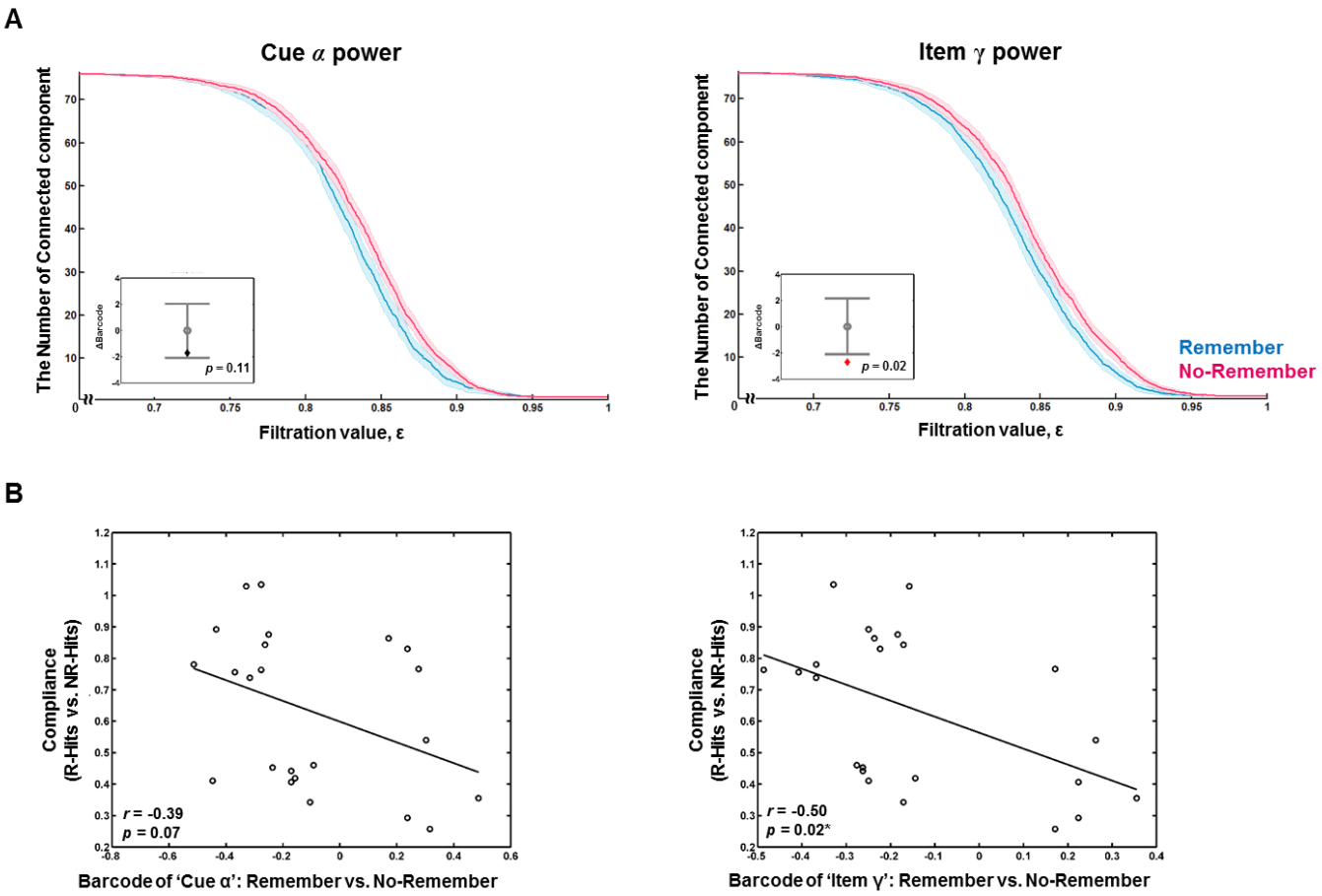
A
Cue α power
Item γ power
The Number of Connected component
Filtration value, ε
ΔBarcode
p = 0.11
p = 0.02
Remember
No-Remember
B
Compliance (R-Hits vs. NR-Hits)
r = -0.39
p = 0.07
r = -0.50
p = 0.02*
Barcode of 'Cue α': Remember vs. No-Remember
Barcode of 'Item γ': Remember vs. No-Remember

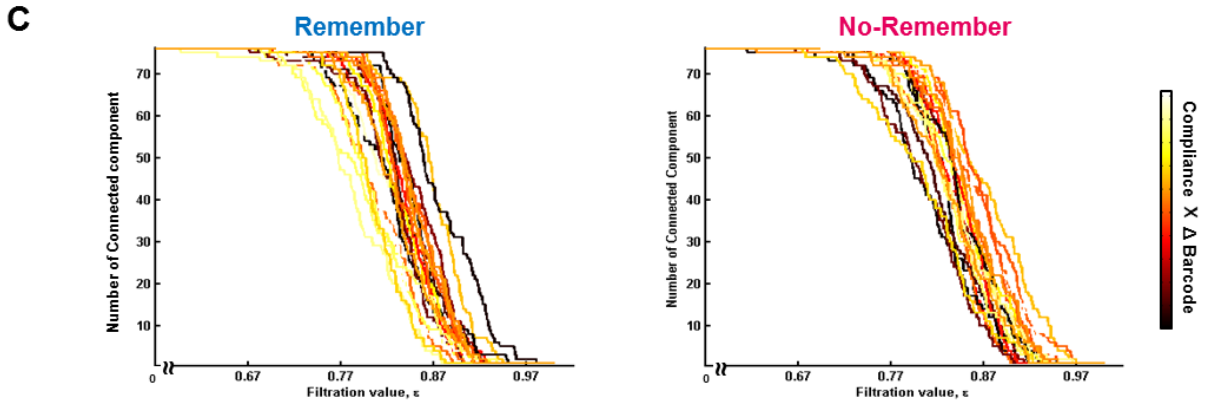

Figure 5. Comparison of barcodes between "Remember" and "No-Remember" conditions for each task phases. After graph filtration, the barcode showed the changes in the formation of connected component across brain-wide regions, reflecting changes in large-scale regional integration. A) Across filtration values, the mean of the number of connected component was displayed and its standard deviation was shown by shade around the line. The barcodes were colored in blue for "Remember" and pink for "No-remember" condition. B) The barcode differences between task conditions were tested to explain the variance of task compliance for each alpha power during cue presentation ('cue alpha') (Left) and gamma power during item presentation ('item gamma') (Right). For the 'item gamma', the difference of barcode between conditions showed significantly negative correlation with task compliance (i.e., R-Hits vs. NR-Hits) (r = -0.50, p = 0.02). This finding was visualized in form of barcode in C). Color indicated interaction between compliance and barcode differences between conditions. Yellowish color reflected an individual who showed faster regional integration in "Remember" than in "No-Remember" condition, and showed good performance in task compliance.

In fact, barcode for each condition showed the changes in the connected component which is defined by the connectivity between ‘cue alpha’ and ‘item gamma’ as a bipartite graph. Hence, to understand the difference in barcodes for ‘item gamma’ shown in Figure 5, the comparison of barcodes was need between ‘cue alpha’ and ‘item gamma’ barcode for each condition. For both the “Remember” and “No-Remember” condition, the mean of barcode for ‘cue alpha’ showed more regions forming connected components than that for ‘item gamma’ (Figure 6A) and showing significant difference in the barcodes between ‘cue alpha’ and ‘item gamma’ (“Remember” condition: $t_{(22)}$ = -2.23, p = 0.04, permutation; “No-Remember” condition: $t_{(22)}$ = -3.27, p =0.003, permutation).

Further, the difference of barcodes between ‘cue alpha’ and ‘item gamma’ explained the variance of memory performance for “Remember” condition (r = -0.50, p = 0.02) (Figure 6B, Left), however “No-Remember” condition did not show any relationship with memory performance (r = -0.07, p = 0.75) (Figure 6B, Right). In fact, memory performance was defined by R-Hits vs False alarms (“New” items), so

that it might not be relevant for “No-Remember” condition. Thus, I made other performance measures such as NR-Hits vs NR-Misses, but none of behavior measure was explained by the difference of the barcode significantly.

Further, the relationship between barcode in the “Remember” condition and memory performance was investigated (Figure 6C). A good performer showed regions of ‘cue alpha’ were merged faster than that of ‘item gamma.’ And it was shown by plotting nodes forming the connected component consisting of more than one node. As expected, more nodes (i.e., regions) were found in ‘cue alpha’ than ‘item gamma’ region. For the largest connected component (i.e., the component comprised of the most number of regions), the percentage of the number of regions belonging to the largest component relative to the total number of regions was 86.84 % and 59.21 %, respectively. On the other hand, a poor performer showed reverse pattern, i.e., more regions were found in ‘item gamma’ (51.32 %) than those in ‘cue alpha’ (71.05 %). These findings demonstrated that $m : n$ (where $m > n$) between ‘cue alpha’ and ‘item gamma’ interaction is predictive of good

memory performance in “Remember” condition.

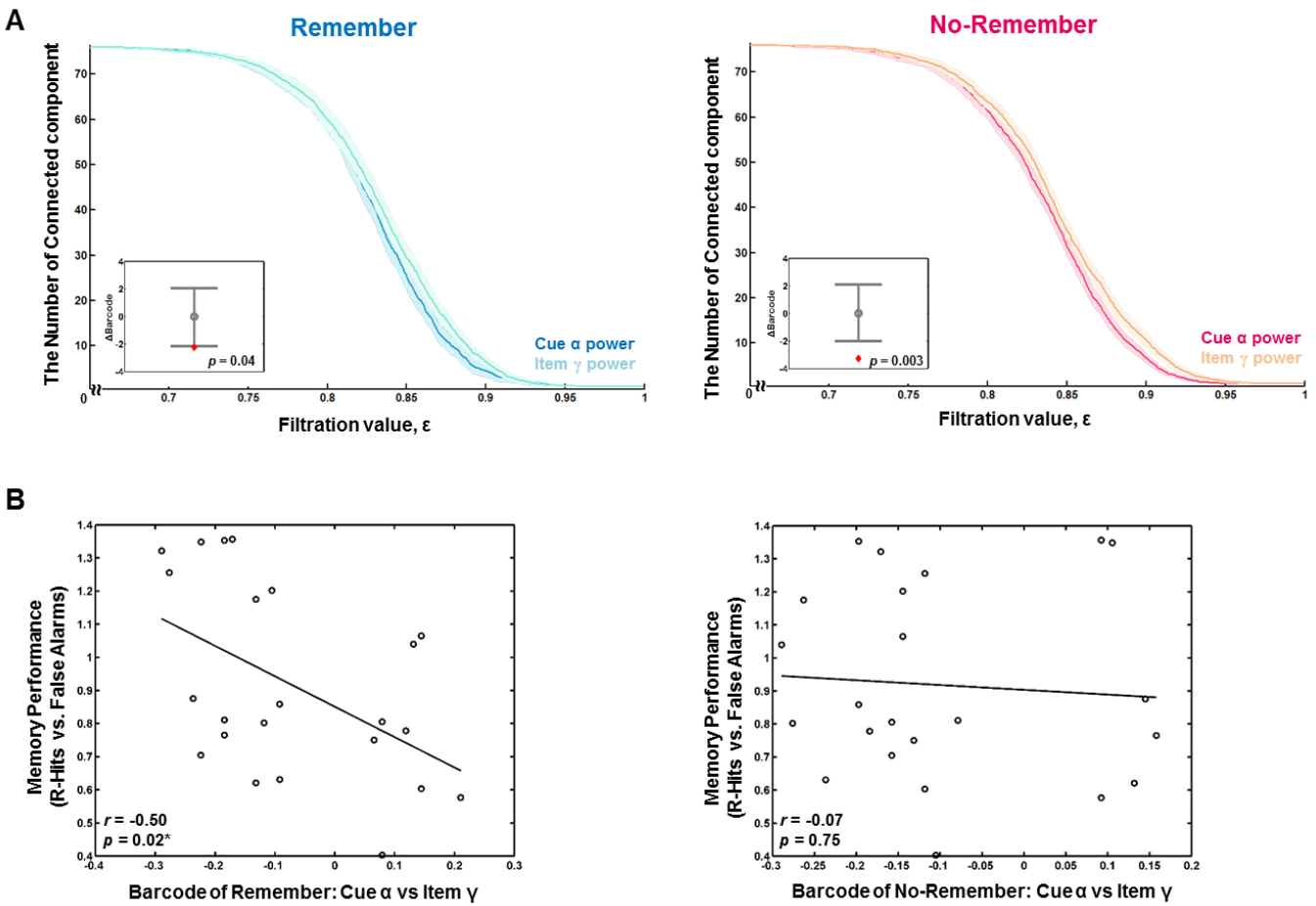
A
Remember
No-Remember
The Number of Connected component
Filtration value, ε
Cue α power
Item γ power
ΔBarcode
p = 0.04
p = 0.003
B
Memory Performance
(R-Hits vs. False Alarms)
r = -0.50
p = 0.02*
r = -0.07
p = 0.75
Barcode of Remember: Cue α vs Item γ
Barcode of No-Remember: Cue α vs Item γ

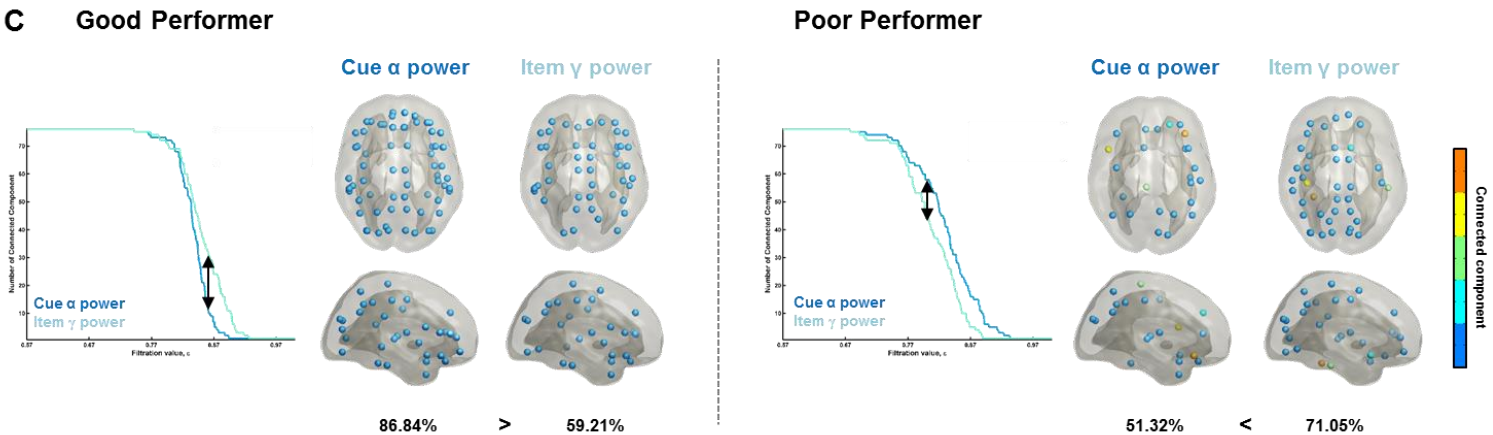

Figure 6. Comparison of Barcodes between 'cue alpha' and 'item gamma' for each task conditions. A) The mean of barcode for alpha power during cue ('cue alpha') showed less connected component than that for gamma power during item ('item gamma') for each condition across filtration values. The barcodes within each condition was significantly different for each condition. B) In "Remember" condition, the maximum distance of barcodes between 'cue alpha' and 'item gamma' was negatively correlated with memory performance (r = -0.50, p = 0.02) (Left). For "No-Remember" condition, it did not show any relationship with memory performance (r = -0.07, p = 0.75) (Right). C) For the "Remember" condition, a good performer shoed more larger regional integration for 'cue alpha' than 'item gamma' while a poor performer showed reverse pattern. This pattern was displayed on the brain, where the connected component consisting of more than one node was displayed as colored regions (which was presented as a sphere in the figure of brain). The one largest connected component was colored in deep blue for both selected subjects. For the largest component, the percentage of the number of nodes was shown on the bottom of the brain.

3.3. Local network property measured by single linkage distance

While the barcode represented the global property of network, the single linkage dendrogram showed local edge contributed to task condition difference. After single linkage dendrogram was converted to SLM, two conditions were compared to each other at every edge (See Figure 4). I found the significant edges between the left insula of item gamma region and each cue alpha region of four: the left temporal pole of superior temporal gyrus (TP.STG), the supramarginal gyrus, the dorsolateral part and the orbital part of the superior frontal gyrus (SFG.dl and SFG.orb), and also between the right middle temporal gyrus (MTG) of cue alpha region and the left orbital part of the middle frontal gyrus (MFG.orb) of item gamma region at $p < 0.0005$, permutation, uncorrected for multiple comparisons (Figure 7A and B, Table 2).

Further, I tested whether those significant edges explain the variance of task compliance. The edge between the left SFG.dl of ‘cue alpha’ and the left insula of ‘item gamma’ showed positive correlation significantly ($r = -0.48$, $p = 0.02$) (Figure 7C). Participants who had

shorter distance between those two nodes in “Remember” than “No-Remember” condition showed better compliance. The superior frontal gyrus was overlapped with the dorsal attention network (Corbetta & Shulman 2002), suggesting the top-down attentional control to encoding. Moreover, this edge showed significance when using the functional connectivity method of the previous study (r = -0.57, p = 0.004) (Figure 7D). In other words, an individual with strong alpha power during cue presentation in “No-Remember” condition had lower gamma power during item in “Remember” condition. This functional connectivity analysis was done for the other edges of four, yielding negative correlation was found in connectivity of the left insula of ‘item gamma’ with the left TP.STG (r = -0.42, p = 0.05), with the left supramarginal gyrus of ‘cue alpha’ (r = -0.44, p = 0.03) (Table 2). Considering this functional connectivity analysis was the same as that shown in the previous work, these results indicated that if the previous work had done for inter-regional connectivity, these edges would have been revealed.

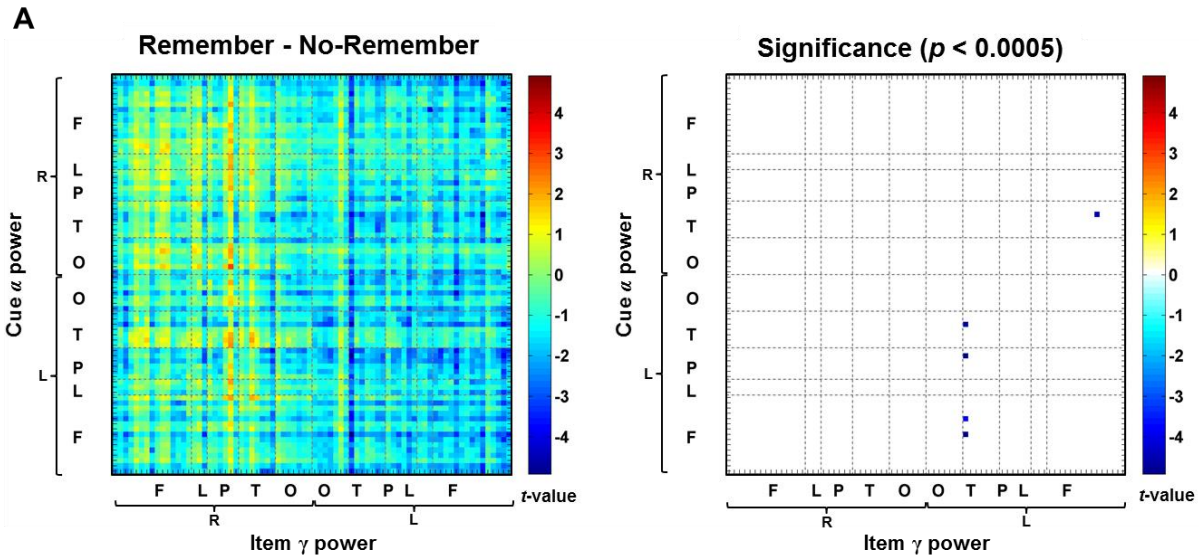
A
Remember - No-Remember
Significance ($p < 0.0005$)
Cue α power
Item γ power
R
L
F L P T O O T P L F
4 3 2 1 0 -1 -2 -3 -4
t-value

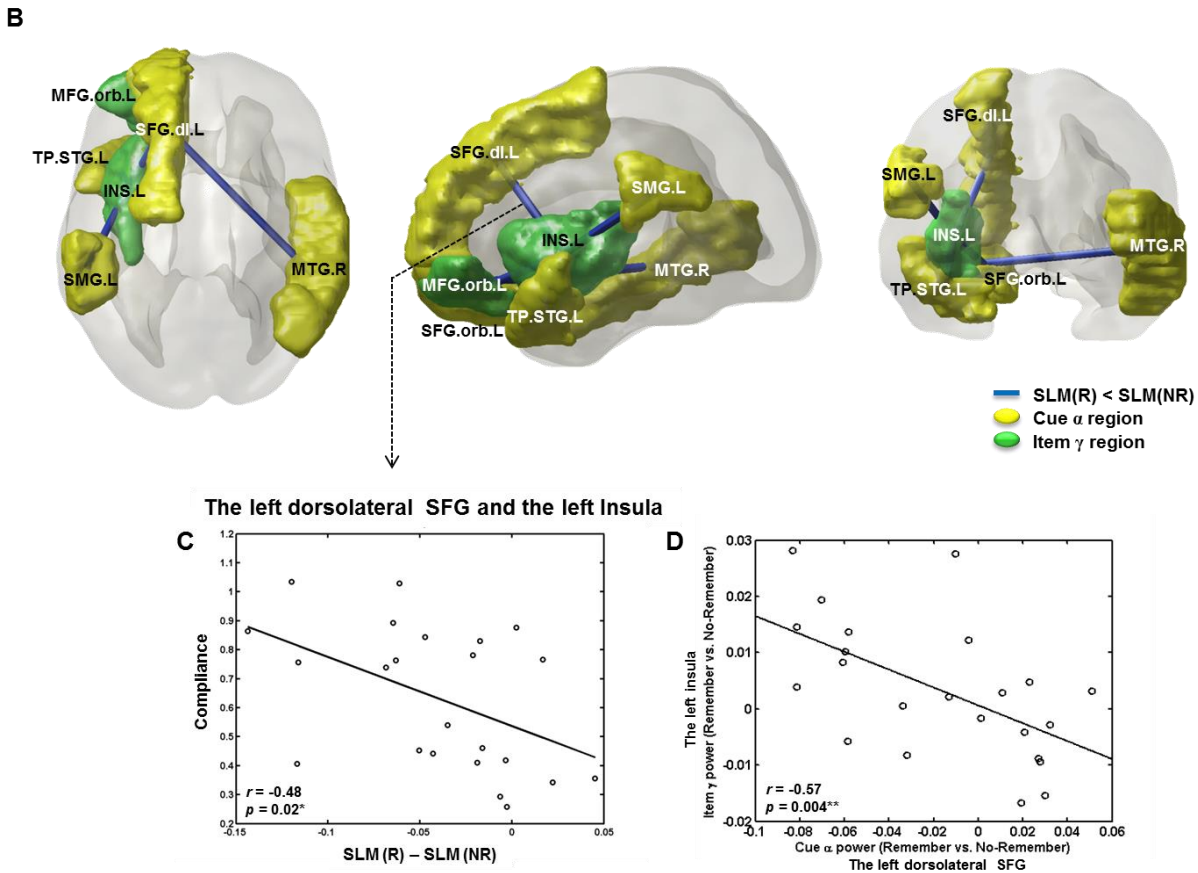
B
MFG.orb.L
SFG.dl.L
TP.STG.L
INS.L
SMG.L
MTG.R
SFG.dl.L
SMG.L
INS.L
MTG.R
MFG.orb.L
TP.STG.L
SFG.orb.L
SFG.dl.L
SMG.L
INS.L
MTG.R
TP.STG.L
SFG.orb.L
SLM(R) < SLM(NR)
Cue α region
Item γ region
The left dorsolateral SFG and the left Insula
C
Compliance
r = -0.48
p = 0.02*
SLM (R) – SLM (NR)
D
The left Insula
Item γ power (Remember vs. No-Remember)
r = -0.57
p = 0.004**
Cue α power (Remember vs. No-Remember)
The left dorsolateral SFG

Figure 7. Differences in single linkage distance between "Remember" and "No-Remember" conditions. A) The t-values between two conditions was shown on the left and its significance at $p < 0.0005$ was displayed on the right side of the figure. The significant distances between conditions were listed in Table 2. B) The significant differences between conditions were displayed on the brain. C) For those significant edges, the difference of single linkage distance between two conditions was correlated with task compliance. Task compliance showed a significant correlation with the edges between the left dorsolateral superior frontal gyrus of the alpha power during cue presentation and the left insula of the gamma power during item presentation ($r = -0.48$, $p = 0.02$). D) Also, this edge exhibited negative cross-frequency correlation of power difference between conditions.

Table 2. The single linkage distance showing significant difference between conditions.

Pair of Relationship		*t*-value (df = 22)	Correlation with compliance	Cross-frequency Correlation of Power difference (R vs NR)
Cue alpha power during cue presentation	**Item gamma power during item presentation**			
Temporal pole: superior temporal gyrus (L)	Insula (L)	-4.57***	-0.24	-0.42*
Supramarginal gyrus (L)		-4.92***	-0.19	-0.44*
Superior frontal gyrus, dorsolateral (L)		-3.93***	-0.48*	-0.57**
Superior frontal gyrus, orbital part (L)		-4.89***	-0.31	-0.38
Middle temporal gyrus (R)	Middle frontal gyrus, orbital part (L)	-4.60***	-0.25	0.03

*p < 0.05, **p < 0.005, ***p < 0.0005, uncorrected for multiple comparisons.

(L): Left, (R): Right
R vs NR: "Remember" condition vs "No-Remember" condition

4. Discussion

The present study examined that large-scale network for encoding regulation by constructing a large-scale network using bipartite graph filtration based on alpha and gamma cross-frequency power interactions. I found that, first, the global characteristics of network reflected by a barcode showed difference between conditions during encoding phase. And the stronger large-scale regional integration during encoding phase in “Remember” than “No-Remember” condition were predictive of task compliance. Also, asymmetric configuration of interaction for encoding regulation reflected by alpha and gamma power correlation was predictive of memory performance. These findings suggested that the large-scale regional integration is predictive of ongoing functional state. Second, the local network features shown by single linkage matrix found that the distance between the left dorsolateral part of superior frontal gyrus and the left insular cortex was significantly closer in “Remember” than

"No-Remember" condition, and which was predictive of task performance. Considering superior frontal gyrus was overlapped in dorsal attention network, it was consistent with the previous work, while the present study found distant inter-regional relationship. The findings suggests that top-down attentional control open a gate to encoding process in the left insular cortex. Here, to investigate how prior information modulate later encoding regulation, bipartite graph filtration was designed for MEG network study for the first time. By measuring cross-time and cross-frequency interactions, bipartite graph filtration approach is suggested to bring the functional brain network one step closer to multi-dimensional network modeling covering interactions among spatio-temporo-spectral dimension.

4.1. Multi-scale connectivity pattern for encoding regulation is distinctive of functional state

I analyzed the global connectivity changes reflected by the shape of barcode in that global connectivity patterns represent functional state. The barcode demonstrated that the changes of global

connectivity was distinctive between task conditions and was predictive of better performance. It supported the “neural context” wherein the functional relevance of a neural element for cognitive function is defined by interaction with other elements (Bressler & McIntosh 2007, Engel 2012, McIntosh 2008). Also the higher cognition such as attention and memory has been suggested to be emerged by large-scale integration (McIntosh 2008, Mesulam 1990, Varela et al 2001). Through interactions of neural populations, the elementary functions integrate with other regions, forming aggregates of neuronal population to represent cognitive function (McIntosh 2008).

Regardless of task conditions, the regions of ‘alpha power’ showed tendency of large scale regional interaction than that of ‘gamma power’. This finding is consistent with the properties of oscillation that higher frequency oscillations are confined to a small neuronal space, whereas slow oscillations recruit very large networks (Csicsvari et al 2003, Kopell et al 2000, Lisman & Idiart 1995, Steriade 2001, von Stein & Sarnthein 2000).

4.2. Top-down controls for encoding in insular cortex is predictive of better performance

Note that the connectivity results was not corrected for multiple comparisons. Rather I focused on the edges hierarchically. First I found the significant edges at $p < 0.0005$ without multiple comparison correction. Then, for the edges found, I focused on the edges showing either significant correlation ($p < 0.05$) with behavioral performance or showing significant functional connectivity ($p < 0.05$) when using the method of the previous study. Finally three connectivity were taken into consideration and discussed.

Three connectivity was between the left insula during encoding phase and each of the left SFG.dl, STG.TP, and supramarginal gyrus during cue interval. As for the superior frontal gyrus, it is overlapped with the dorsal attentional network indicating top-down control (Corbetta & Shulman 2002), which is in line with the previous study demonstrating top-down attentional control by alpha power (Park et al 2014), although the region was not consistent. As for the left supramarginal gyrus, it has been suggested to be a player for bottom-up

attentional processing as a part of the ventral parietal cortex (Cabeza et al 2012, Corbetta & Shulman 2002). In fact, the cue presentation instructed the task for forthcoming phase, so that subjects anticipate and prepare for the next phase by top-down control. However during cue presentation there was not empty since the fixation cross was presented. Thus the cue information might be salient enough to capture attention through bottom-up process. Thus in this study, both top-down and bottom-up process might be involved during cue presentation. In addition, the bottom-up attention has been demonstrated to be one mechanism facilitating encoding (Ravizza & Hazeltine 2013), suggesting its relationship with later encoding processing is possible. As for the temporal pole at the superior temporal gyrus, it have shown to have relationship with the insula as a component of the salience network (Seeley et al 2007). As for the insular cortex, it has shown to be involved in memory function, specifically in acquisition and consolidation (Bermudez-Rattoni et al 2005, Chen et al 2009). Recent study have demonstrated that the functional network of the insula is important for memory function (Xie et al 2012). In addition,

Considering the insular cortex has been suggested as an integral hub to facilitate access to attention and memory by mediating between bottom-up and top-down attention control (Menon & Uddin 2010), the finding suggested that the left insular cortex integrate both top-down process in the SFG.dl and bottom-up process in the supramarginal gyrus.

Among these connectivity, connectivity only between the left superior frontal gyrus and the left insula was related to the task performance, suggesting top-down control via the SFG.dl over later encoding in the insula is relevant to task performance. It was consistent with the documented findings in terms of memory function. For the superior frontal cortex, it is not only for attentional control, but also shown to be involved in memory function (du Boisgueheneuc et al 2006, Rypma et al 1999). And for the connectivity between superior frontal gyrus and insula, the variance of it was explained by memory score in patients with mild cognitive impairment when examined by resting-state functional coupling using BOLD signal (Xie et al 2012). Considering the relationship was closer in “Remember” condition than in “No-Remember” condition (Figure 8C), better task performance can

be explained by decrease in alpha power in the SFG.dl open gates to the insular cortex by increase in gamma power.

4.3. The estimation of interaction between alpha and gamma band power

While the previous study found alpha and gamma functional connectivity in posterior region (Park et al 2014), the present study could not found significant connectivity in the precuneus. One explanation is the difference in connectivity metric between the previous study and the current one regardless of graph filtration method. The functional connectivity method of the previous study reveals changes in power correlation with respect to task condition, like psychophysiological interaction (Friston et al 1997). This method has been reported as a method for examining functional connectivity (Mazaheri et al 2009). The functional connectivity method of the previous study was performed by calculating correlation coefficient between the difference of alpha power between conditions and the difference of gamma power between conditions, yielding the negative

correlation in the bilateral precuneus. On the other hand, the current study aimed to examine cross-frequency power interaction for each task condition at individual network by estimating regional relationship across trials. This method was similar to that used in other studies (Brookes et al 2011a, Bruns et al 2000, Mazaheri et al 2010, Park et al 2011). However, this method did not showed the precuneus as a region with strong power correlation as shown in the previous study. The method used in the present study considered cross-frequency power interaction at the single trial level, while the functional connectivity method of the previous study dealt with the difference in the average of power over trials between conditions.

In fact there are a variety of connectivity measures in electrophysiological data, such as power correlation, mutual information, phase synchronization, and so on (Greenblatt et al 2012). Several studies suggested that the different connectivity measure can be complementary to each other for better understanding on the electrical nature of brain functional connectivity (Brookes et al 2011a, Bruns et al 2000). In this sense, I suggested that each connectivity metric indicate

different aspect of electrophysiological connectivity engaged in encoding regulation by prior information.

4.4. Graph filtration method for investigating brain network structure

In the current study, I applied the graph filtration method for the reason as follows. First, as described above, this method is threshold-free, avoiding any arbitrary selection of threshold or possibility of information loss. Moreover, it provides the invariant measure of network, such as barcode and single linkage dendrogram. Second, it has been suggested to be appropriate for an exploratory study (Singh et al 2008). In fact the present study had no any assumption on global or regional connectivity pattern in particular. Third, it has been suggested to be plausible to elucidate the basic structure of biological data. For example, Singh et al. (2008) reported that the method exhibited similar topological feature between the spontaneous neuronal population activity and the activity driven by natural image sequence in primary visual cortex. The finding was

consistent with the previous documented results, suggesting that the topological analysis help to uncover the underlying structure of neural activity. Further, topological structure of large-scale brain network has been revealed by the graph filtration method in pathological human (Kim et al 2014, Lee et al 2012) and rodent model (Choi et al 2014, Khalid et al 2014), suggesting invariant features from graph filtration is good tools to reveal underlying structure of the pathological brain network.

In the present study, topological changes were examined by a barcode and single linkage matrix using graph filtration method. The barcode indicated that the cognitive function can be captured by interaction patterns among regions. And the single linkage matrix found the significant connectivity related in memory regulation, indicating the performance of graph filtration as an exploratory analysis method.

4.5. Modeling a large-scale network in cerebral cortex using electrophysiological data

Most of studies on oscillatory power have been examined by focusing on local regional increase or decrease in oscillatory power. However, information processing in the cerebral cortex has been suggested to be obtained by interactions among distributed cortical modules covering large-scale regions as suggested in the rodent brain study (Oh et al 2014). Also it has been suggested to work through spatiotemporal dimension as well (Engel et al 2013). Thus functional brain network needs to be modeled in terms of multi-dimensional interactions for understanding brain network better. In this sense, the present study expand the spatial dimension of cross-time and cross-frequency interactions by constructing large-scale network using bipartite graph filtration as the first step of a multi-dimensional network construction.

The exploratory network analysis has been reported in several eletrophysiological studies using seed-based approach (de Pasquale et al 2010), or using independent component analysis (Brookes et al 2011b), or by computing all-to-all statistical dependency on source level (Hipp et al 2011, Hipp et al 2012, Palva & Palva 2011, Tewarie et

al 2014). Since there was no correct answer for brain network approach, I used graph filtration, one promising method, after modeling bipartite graph for time lagged and cross-frequency data analysis for the first time.

The limitation of the present study in terms of network construction was as follows. For network construction, definition of node and edge is of importance. For the node definition, , I used AAL atlas by excluding subcortical and cerebellar brain structures like Tewarie et al (2014) for an MEG brain network study. In fact, AAL atlas parcellated the regions based on anatomical information based on a single subject brain (Tzourio-Mazoyer et al 2002). Also thirty-eight regions covering each hemisphere are not sufficient to be a representative of functional unit in the cerebral cortex since it regards a single gyrus as a single node while one gyrus can be divided by several sub-regions according to its specific function. For the edge definition, the present study estimated correlation coefficient between regions. The correlation coefficient did not show any causality. Thus noted that, it is hard to mention a causal relationship between attentional control and

encoding although the cue preceded the item.

5. Conclusion

In conclusion, encoding regulation is operated by large scale regional interactions. The different state of memory regulation and corresponding memory performance depends on configuration of the large-scale integration between alpha and gamma oscillatory power. Finally the opening gate by top-down attentional control for later encoding process in the insular cortex helps better memory performance. Considering the brain works in multiple dimensions including spatio-temporal-spectral dimension, the present study reach first base with the multi-dimensional analysis. In the future, modeling multi-dimensional interaction is needed to elucidate the neural mechanism of how brain function further.

“Remember” vs “No-Remember” condition

Cue α (10Hz) power during cue presentation

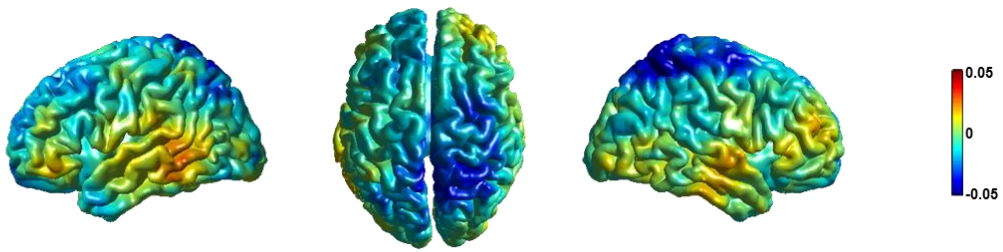

Item γ (80Hz) power during item presentation

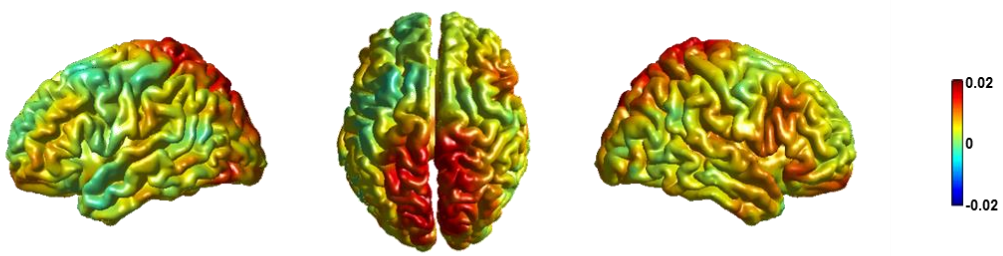

Supplementary Figure 1. The comparison of the source spectral power after normalization based on the inter-trial interval. In the present study, I aimed to construct a network for each task condition at single trial level. To do this, I normalized each spectral power source of 10 Hz during cue presentation (latency 1 s) and of 80 Hz during item presentation (latency 1 s) by dividing a mean value of the source power in each presentation latency and the inter-trial interval (latency 1 s). The figure showed grand average (N = 23) of differences in power spectrum between task conditions ("Remember" vs "No-Remember" condition). The stronger alpha power during cue and weaker gamma power during item in "No-Remember" than "Remember" condition, especially in the posterior region, as shown in our previous study albeit the normalization method was different from those in the previous study.

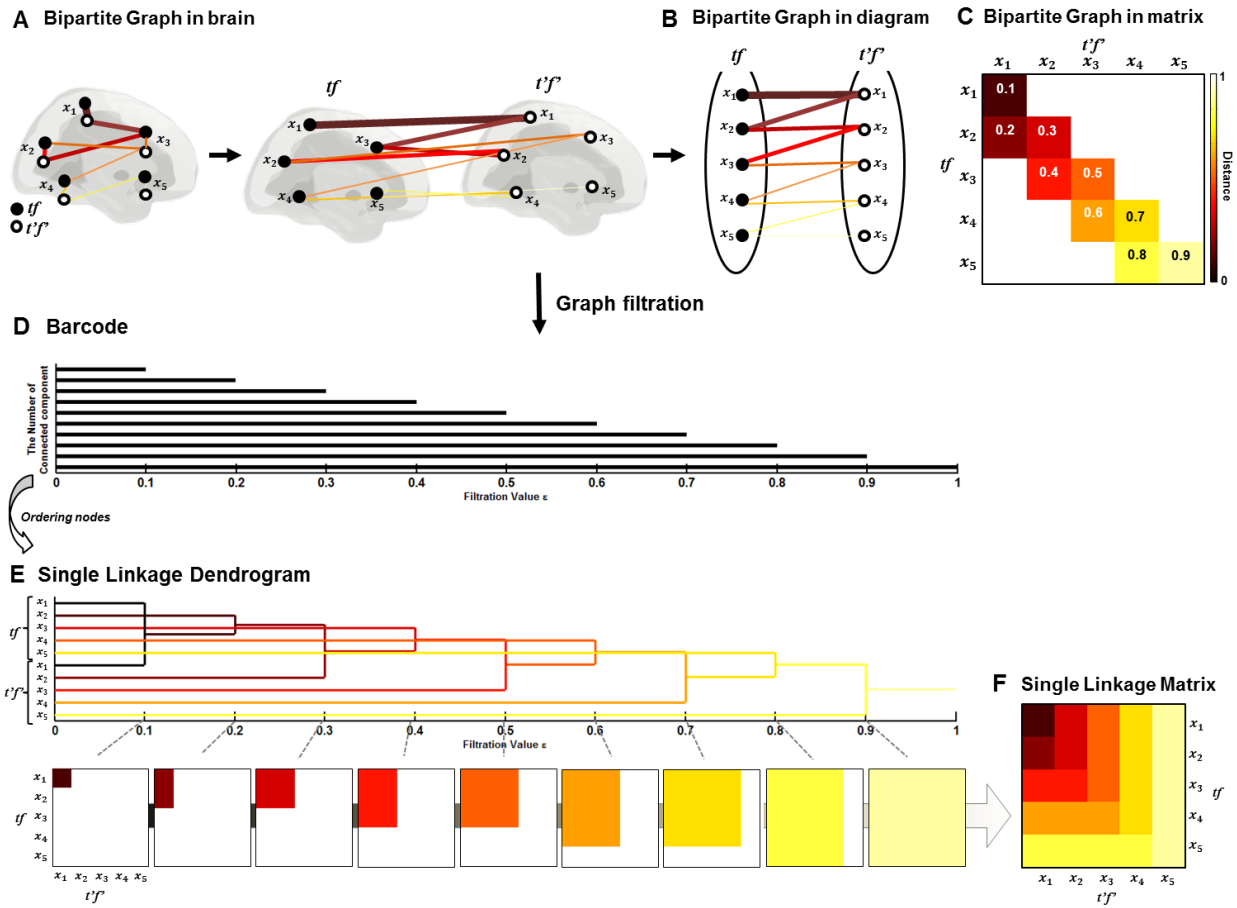
A Bipartite Graph in brain
B Bipartite Graph in diagram
C Bipartite Graph in matrix
tf
t'f'
Graph filtration
D Barcode
The Number of Connected component
Filtration Value ε
Ordering nodes
E Single Linkage Dendrogram
F Single Linkage Matrix
Distance

Supplementary Figure 2. Graph filtration for bipartite graph. A) The example of bipartite graph was shown with different connectivity strength. The bipartite graph consisted of a node set of time (*t*) and frequency (*f*) and a set of different time (*t'*) and frequency (*f'*). B) The bipartite graph was presented in diagram for simplification of the display. The strength (i.e. distance) of connectivity in bipartite graph was assigned from 0.1 to 0.9 with incremental 0.1. C) The distance between nodes in bipartite can be displayed in matrix. D) As the filtration goes from 0 to 1, the size of connected component grows while the number of connected component reduced one by one. E) To find any regionally significant distance in barcode, single linkage dendrogram was generated by ordering the label of barcode. F) To test dendrogram, the single linkage distance was transformed into a matrix form, yielding single linkages matrix.

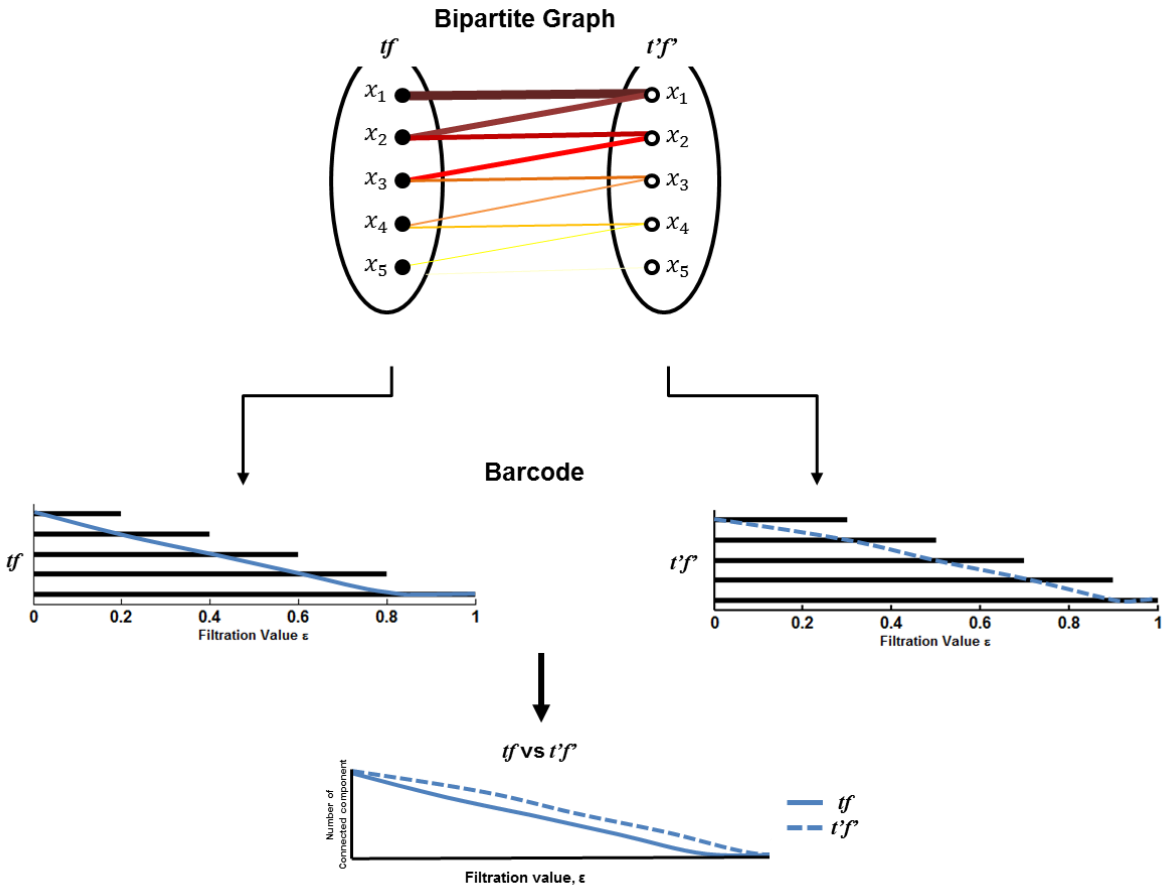
Bipartite Graph
tf
t'f'
x_1
x_2
x_3
x_4
x_5
Barcode
tf
t'f'
0
0.2
0.4
0.6
0.8
1
Filtration Value ε
tf vs t'f'
Number of Connected component
Filtration value, ε
tf
t'f'

Supplementary Figure 3. Barcode separation for bipartite graph. Especially, the barcode of bipartite graph can be divided into two barcodes for each set of nodes. Then, the barcode is represented by the line by linking dots at every death filtration value of connected component (blue line). The lines from two sets of nodes can be plotted together, showing the difference between barcodes. The barcode of *tf* had less number of connected component than that of *t'f'* since two sets of nodes were linked by two nodes of *tf* and one node of *t'f'* (2 : 1). Thus comparison of barcodes in bipartite graph can reveal the pattern of interconnectivity between sets.

References

Ai L, Ro T. 2014. The phase of prestimulus alpha oscillations affects tactile perception. *J Neurophysiol* 111: 1300-7

Anderson MC, Green C. 2001. Suppressing unwanted memories by executive control. *Nature* 410: 366-9

Anderson MC, Levy BJ. 2009. Suppressing Unwanted Memories. *Current Directions in Psychological Science* 18: 189-94

Anderson MC, Ochsner KN, Kuhl B, Cooper J, Robertson E, et al. 2004. Neural systems underlying the suppression of unwanted memories. *Science* 303: 232-5

Bassett DS, Nelson BG, Mueller BA, Camchong J, Lim KO. 2012. Altered resting state complexity in schizophrenia. *Neuroimage* 59: 2196-207

Bennett MV, Zukin RS. 2004. Electrical coupling and neuronal synchronization in the Mammalian brain. *Neuron* 41: 495-511

Bermudez-Rattoni F, Okuda S, Roozendaal B, McGaugh JL. 2005. Insular cortex is involved in consolidation of object recognition memory. *Learn Memory* 12: 447-49

Bressler S, McIntosh A. 2007. The Role of Neural Context in Large-Scale Neurocognitive Network Operations In *Handbook of Brain Connectivity*, ed. V Jirsa, AR McIntosh, pp. 403-19: Springer Berlin Heidelberg

Bressler SL. 1995. Large-scale cortical networks and cognition. *Brain Res Brain Res Rev* 20: 288-304

Bressler SL, Coppola R, Nakamura R. 1993. Episodic multiregional cortical coherence at multiple frequencies during visual task performance. *Nature* 366: 153-6

Bressler SL, Tognoli E. 2006. Operational principles of neurocognitive networks. *Int J Psychophysiol* 60: 139-48

Brookes MJ, Hale JR, Zumer JM, Stevenson CM, Francis ST, et al. 2011a. Measuring functional connectivity using MEG: methodology and comparison with fcMRI. *Neuroimage* 56: 1082-104

Brookes MJ, Woolrich M, Luckhoo H, Price D, Hale JR, et al. 2011b. Investigating the electrophysiological basis of resting state networks using magnetoencephalography. *Proc Natl Acad Sci U S A* 108: 16783-8

Bruns A, Eckhorn R, Jokeit H, Ebner A. 2000. Amplitude envelope correlation detects coupling among incoherent brain signals. *Neuroreport* 11: 1509-14

Bullmore E, Sporns O. 2009. Complex brain networks: graph theoretical analysis of structural and functional systems. *Nat Rev Neurosci* 10: 186-98

Bullmore ET, Bassett DS. 2011. Brain graphs: graphical models of the human brain connectome. *Annual review of clinical psychology* 7: 113-40

Burianova H, Ciaramelli E, Grady CL, Moscovitch M. 2012. Top-down and bottom-up attention-to-memory: mapping functional connectivity in two distinct networks that underlie cued and uncued recognition memory. *Neuroimage* 63: 1343-52

Buzsaki G, Watson BO. 2012. Brain rhythms and neural syntax: implications for efficient coding of cognitive content and neuropsychiatric disease. *Dialogues in clinical neuroscience* 14: 345-67

Cabeza R, Ciaramelli E, Moscovitch M. 2012. Cognitive contributions of the ventral parietal cortex: an integrative theoretical account. *Trends Cogn Sci* 16: 338-52

Chen SL, Li LJ, Xu BH, Liu J. 2009. Insular cortex involvement in declarative memory deficits in patients with post-traumatic stress disorder. *Bmc Psychiatry* 9

Choi H, Kim YK, Kang H, Lee H, Im HJ, et al. 2014. Abnormal metabolic connectivity in the pilocarpine-induced epilepsy rat model: A multiscale network analysis based on persistent homology. *Neuroimage* 99: 226-36

Chun MM, Turk-Browne NB. 2007. Interactions between attention and memory. *Current Opinion in Neurobiology* 17: 177-84

Ciaramelli E, Grady CL, Moscovitch M. 2008. Top-down and bottom-up attention to memory: a hypothesis (AtoM) on the role of the posterior parietal cortex in memory retrieval. *Neuropsychologia* 46: 1828-51

Corbetta M, Shulman GL. 2002. Control of goal-directed and stimulus-driven attention in the brain. *Nat Rev Neurosci* 3: 201-15

Csicsvari J, Jamieson B, Wise KD, Buzsaki G. 2003. Mechanisms of gamma oscillations in the hippocampus of the behaving rat. *Neuron* 37: 311-22

de Pasquale F, Della Penna S, Snyder AZ, Lewis C, Mantini D, et al. 2010. Temporal dynamics of spontaneous MEG activity in brain networks. *Proc Natl Acad Sci U S A* 107: 6040-5

Depue BE, Curran T, Banich MT. 2007. Prefrontal regions orchestrate suppression of emotional memories via a two-phase process. *Science* 317: 215-9

Destexhe A, Contreras D, Steriade M. 1999. Spatiotemporal analysis of local field potentials and unit discharges in cat cerebral cortex during natural wake and sleep states. *J Neurosci* 19: 4595-608

du Boisgueheneuc F, Levy R, Volle E, Seassau M, Duffau H, et al.

2006. Functions of the left superior frontal gyrus in humans: a lesion study. *Brain* 129: 3315-28

Engel Andreas K. 2012. Rules Got Rhythm. *Neuron* 76: 673-76

Engel AK, Gerloff C, Hilgetag CC, Nolte G. 2013. Intrinsic coupling modes: multiscale interactions in ongoing brain activity. *Neuron* 80: 867-86

Freunberger R, Fellinger R, Sauseng P, Gruber W, Klimesch W. 2009. Dissociation between phase-locked and nonphase-locked alpha oscillations in a working memory task. *Hum Brain Mapp* 30: 3417-25

Fries P, Reynolds JH, Rorie AE, Desimone R. 2001. Modulation of oscillatory neuronal synchronization by selective visual attention. *Science* 291: 1560-3

Friston KJ, Buechel C, Fink GR, Morris J, Rolls E, Dolan RJ. 1997. Psychophysiological and modulatory interactions in neuroimaging. *Neuroimage* 6: 218-29

Gazzaley A. 2011. Influence of early attentional modulation on working memory. *Neuropsychologia* 49: 1410-24

Gevins A, Morgan N, Bressler S, Cutillo B, White R, et al. 1987. Human neuroelectric patterns predict performance accuracy. *Science* 235: 580-85

Greenblatt RE, Pflieger ME, Ossadtchi AE. 2012. Connectivity measures applied to human brain electrophysiological data. *J Neurosci Methods* 207: 1-16

Gross J, Baillet S, Barnes GR, Henson RN, Hillebrand A, et al. 2013. Good practice for conducting and reporting MEG research. *Neuroimage* 65: 349-63

Gross J, Kujala J, Hamalainen M, Timmermann L, Schnitzler A, Salmelin R. 2001. Dynamic imaging of coherent sources: Studying neural interactions in the human brain. *Proc Natl*

Acad Sci U S A 98: 694-9

Haegens S, Osipova D, Oostenveld R, Jensen O. 2010. Somatosensory working memory performance in humans depends on both engagement and disengagement of regions in a distributed network. *Hum Brain Mapp* 31: 26-35

Hanslmayr S, Leipold P, Bauml KH. 2010. Anticipation boosts forgetting of voluntarily suppressed memories. *Memory* 18: 252-7

Hanslmayr S, Leipold P, Pastotter B, Bauml KH. 2009. Anticipatory signatures of voluntary memory suppression. *J Neurosci* 29: 2742-7

Hipp JF, Engel AK, Siegel M. 2011. Oscillatory synchronization in large-scale cortical networks predicts perception. *Neuron* 69: 387-96

Hipp JF, Hawellek DJ, Corbetta M, Siegel M, Engel AK. 2012. Large-scale cortical correlation structure of spontaneous oscillatory activity. *Nat Neurosci*

Jensen O, Kaiser J, Lachaux JP. 2007. Human gamma-frequency oscillations associated with attention and memory. *Trends Neurosci* 30: 317-24

Jerbi K, Ossandon T, Hamame CM, Senova S, Dalal SS, et al. 2009. Task-Related Gamma-Band Dynamics From an Intracerebral Perspective: Review and Implications for Surface EEG and MEG. *Human Brain Mapping* 30: 1758-71

Johnson JS, Hamidi M, Postle BR. 2010. Using EEG to explore how rTMS produces its effects on behavior. *Brain topography* 22: 281-93

Khalid A, Kim BS, Chung MK, Ye JC, Jeon D. 2014. Tracing the

evolution of multi-scale functional networks in a mouse model of depression using persistent brain network homology. *NeuroImage* 101: 351-63

Kim E, Kang H, Lee H, Lee HJ, Suh MW, et al. 2014. Morphological brain network assessed using graph theory and network filtration in deaf adults. *Hearing Res* 315: 88-98

Kopell N, Ermentrout GB, Whittington MA, Traub RD. 2000. Gamma rhythms and beta rhythms have different synchronization properties. *P Natl Acad Sci USA* 97: 1867-72

Lee H, Chung MK, Kang H, Kim B-N, Lee DS. 2011a. Discriminative persistent homology of brain networks. *ISBI*

Lee H, Chung MK, Kang H, Kim BN, Lee DS. 2011b. Computing the shape of brain networks using graph filtration and Gromov-Hausdorff metric. *Med Image Comput Comput Assist Interv* 14: 302-9

Lee H, Kang H, Chung MK, Kim BN, Lee DS. 2012. Persistent brain network homology from the perspective of dendrogram. *IEEE Trans Med Imaging* 31: 2267-77

Lenartowicz A, McIntosh AR. 2005. The role of anterior cingulate cortex in working memory is shaped by functional connectivity. *J Cogn Neurosci* 17: 1026-42

Lisman JE, Idiart MA. 1995. Storage of 7 +/- 2 short-term memories in oscillatory subcycles. *Science* 267: 1512-5

Maclin EL, Mathewson KE, Low KA, Boot WR, Kramer AF, et al. 2011. Learning to multitask: effects of video game practice on electrophysiological indices of attention and resource allocation. *Psychophysiology* 48: 1173-83

Mazaheri A, Coffey-Corina S, Mangun GR, Bekker EM, Berry

AS, Corbett BA. 2010. Functional disconnection of frontal cortex and visual cortex in attention-deficit/hyperactivity disorder. *Biol Psychiatry* 67: 617-23

Mazaheri A, Nieuwenhuis IL, van Dijk H, Jensen O. 2009. Prestimulus alpha and mu activity predicts failure to inhibit motor responses. *Hum Brain Mapp* 30: 1791-800

McIntosh A. 2008. Large-Scale Network Dynamics in Neurocognitive Function In *Coordination: Neural, Behavioral and Social Dynamics*, ed. A Fuchs, V Jirsa, pp. 183-204: Springer Berlin Heidelberg

McIntosh AR. 1999. Mapping cognition to the brain through neural interactions. *Memory* 7: 523-48

McIntosh AR. 2000. Towards a network theory of cognition. *Neural networks : the official journal of the International Neural Network Society* 13: 861-70

McIntosh AR, Gonzalez-Lima F. 1994. Structural equation modeling and its application to network analysis in functional brain imaging. *Human Brain Mapping* 2: 2-22

Meeuwissen EB, Takashima A, Fernandez G, Jensen O. 2010. Increase in posterior alpha activity during rehearsal predicts successful long-term memory formation of word sequences. *Hum Brain Mapp*

Menon V, Uddin LQ. 2010. Saliency, switching, attention and control: a network model of insula function. *Brain Struct Funct* 214: 655-67

Mesulam MM. 1990. Large-scale neurocognitive networks and distributed processing for attention, language, and memory. *Ann Neurol* 28: 597-613

Oh SW, Harris JA, Ng L, Winslow B, Cain N, et al. 2014. A mesoscale connectome of the mouse brain. *Nature* 508: 207-14

Oostenveld R, Fries P, Maris E, Schoffelen JM. 2011. FieldTrip: Open source software for advanced analysis of MEG, EEG, and invasive electrophysiological data. *Comput Intell Neurosci* 2011: 156869

Palva S, Palva JM. 2011. Functional roles of alpha-band phase synchronization in local and large-scale cortical networks. *Frontiers in psychology* 2: 204

Palva S, Palva JM. 2012. Discovering oscillatory interaction networks with M/EEG: challenges and breakthroughs. *Trends in Cognitive Sciences* 16: 219-30

Park H, Kang E, Kang H, Kim JS, Jensen O, et al. 2011. Cross-frequency power correlations reveal the right superior temporal gyrus as a hub region during working memory maintenance. *Brain connectivity* 1: 460-72

Park H, Lee DS, Kang E, Kang H, Hahm J, et al. 2014. Blocking of irrelevant memories by posterior alpha activity boosts memory encoding. *Human Brain Mapping*: n/a-n/a

Percival DB, Walden AT. 1993. *Spectral Analysis for Physical Applications*. Cambridge University Press.

Pesaran B, Pezaris JS, Sahani M, Mitra PP, Andersen RA. 2002. Temporal structure in neuronal activity during working memory in macaque parietal cortex. *Nat Neurosci* 5: 805-11

Pfurtscheller G, Lopes da Silva FH. 1999. Event-related EEG/MEG synchronization and desynchronization: basic principles. *Clin Neurophysiol* 110: 1842-57

Ravizza SM, Hazeltine E. 2013. The benefits of stimulus-driven attention for working memory encoding. *J Mem Lang* 69: 384-96

Rypma B, Prabhakaran V, Desmond JE, Glover GH, Gabrieli JD.

1999. Load-dependent roles of frontal brain regions in the maintenance of working memory. *Neuroimage* 9: 216-26

Schnitzler A, Gross J. 2005. Normal and pathological oscillatory communication in the brain. *Nat Rev Neurosci* 6: 285-96

Seeley WW, Menon V, Schatzberg AF, Keller J, Glover GH, et al. 2007. Dissociable intrinsic connectivity networks for salience processing and executive control. *J Neurosci* 27: 2349-56

Siegel M, Donner TH, Engel AK. 2012. Spectral fingerprints of large-scale neuronal interactions. *Nat Rev Neurosci* 13: 121-34

Singh G, Memoli F, Ishkhanov T, Sapiro G, Carlsson G, Ringach DL. 2008. Topological analysis of population activity in visual cortex. *Journal of vision* 8: 11 1-18

Sporns O. 2011. The human connectome: a complex network. *Annals of the New York Academy of Sciences* 1224: 109-25

Steriade M. 1997. Synchronized activities of coupled oscillators in the cerebral cortex and thalamus at different levels of vigilance. *Cereb Cortex* 7: 583-604

Steriade M. 2001. Impact of network activities on neuronal properties in corticothalamic systems. *J Neurophysiol* 86: 1-39

Taulu S, Simola J. 2006. Spatiotemporal signal space separation method for rejecting nearby interference in MEG measurements. *Physics in medicine and biology* 51: 1759-68

Taulu S, Simola J, Kajola M. 2005. Applications of the Signal Space Separation Method. *Signal Processing, IEEE Transactions on* 53: 3359-72

Tewarie P, Hillebrand A, Schoonheim MM, van Dijk BW, Geurts

JJG, et al. 2014. Functional brain network analysis using minimum spanning trees in Multiple Sclerosis: An MEG source-space study. *NeuroImage*

Thut G, Miniussi C, Gross J. 2012. The functional importance of rhythmic activity in the brain. *Current biology : CB* 22: R658-63

Tzourio-Mazoyer N, Landeau B, Papathanassiou D, Crivello F, Etard O, et al. 2002. Automated anatomical labeling of activations in SPM using a macroscopic anatomical parcellation of the MNI MRI single-subject brain. *Neuroimage* 15: 273-89

Van Hooff JC, Whitaker TA, Ford RM. 2009. Directed forgetting in direct and indirect tests of memory: seeking evidence of retrieval inhibition using electrophysiological measures. *Brain Cogn* 71: 153-64

Varela F, Lachaux JP, Rodriguez E, Martinerie J. 2001. The brainweb: phase synchronization and large-scale integration. *Nat Rev Neurosci* 2: 229-39

von Stein A, Sarnthein J. 2000. Different frequencies for different scales of cortical integration: from local gamma to long range alpha/theta synchronization. *Int J Psychophysiol* 38: 301-13

Wig GS, Schlaggar BL, Petersen SE. 2011. Concepts and principles in the analysis of brain networks. *Ann N Y Acad Sci* 1224: 126-46

Xie C, Bai F, Yu H, Shi Y, Yuan Y, et al. 2012. Abnormal insula functional network is associated with episodic memory decline in amnestic mild cognitive impairment. *NeuroImage* 63: 320-27

국문 초록

부호화에 대한 주의 조절의 뇌 기능적 신경망: 양분 그래프 필트레이션 기반의 오실레이션 관계 연구

함 자 랑
서울대학교 대학원
인지과학 협동과정

효율적으로 기억하기 위해서는 관련된 정보를 부호화하고 무관한 것은 억제하는 것이 중요하다. 선행 연구에서는 이러한 기억 조절 기능의 신경 상관물로서 뇌 영역 내에서 이루어지는 알파 오실레이션과 감마 오실레이션 간의 상호작용을 제시하였다. 그러나 본 연구에서는 이러한 상호작용을 공간 차원으로 확장하여 기억 조절에 대한 대규모 신경망을 연구하였다.

본 연구에서는, 스물 세 명의 건강한 성인이 '기억'(Remember)과 '비기억'(No-Remember) 단서에 따라 그 다음에 제시되는 사진 자극을 기억하거나 기억하지 마라는 지시를 따르는 동안의 뇌 활동을 뇌자도를 이용하여 측정한 데이터를 분석하였다. 기억 조절에 대한 신경망은 자극 제시 전의 알파 파워와 자극 제시 시의 감마 파워 간의 상호작용을 모든 영역 (즉, 노드) 간의 관계로 구성되었다. 각 노드는 주파수와 시간의 관점에서 두 세트로 나뉠 수 있으며, 이렇게 두 세트의 노드 간의 관계로 이루어진 신경

망을 양분 그래프라고 한다. 이 양분 그래프에 필트레이션 방법을 적용하여 두 노드 간의 연결성에 따른 연결 성분 (connected component)의 변화를 양적으로 변환시켜, 바코드와 단일 접합 거리 (single linkage distance)를 계산하였다. 본 연구에서는 이 방법을 양분 그래프 필트레이션이라 불렀다.

그 결과, 바코드를 통해 살펴본 전체 연결성 패턴에서, 자극 제시 동안의 감마 파워의 전체 영역 간 연결이 기억 조건에서 비기억 조건보다 더 빨리 이루어졌으며 기억 조건에서 더 빨리 이루어질수록 과제 지시를 잘 따르는 경향을 보였다. 또한 기억 조건에서는 단서 제시 동안의 알파 파워에서 연결된 영역의 수가 자극 제시 동안의 감마 파워에서의 수보다 더 많이 나타날수록 기억 수행을 잘 하는 것으로 나타났다. 이러한 결과들은 부호화 조절이 전체 뇌 신경망의 영역 간 상호작용으로 이루어지며 인지 기능의 특성을 영역 간 연결성 패턴으로 설명할 수 있음을 시사한다. 한 편, 단일 접합 거리를 통해 살펴본 국소적인 연결성에서는 단서 제시 동안의 좌측 배외측 상전두 (背外廁 上前頭; dorsolateral superior frontal) 영역과 자극 제시 동안의 좌측 섬피질(insular cortex) 사이의 거리가 유의하게 기억조건이 비기억 조건보다 가깝게 관찰되었으며, 기억조건에서 더 가까울수록 지시에 따른 과제 수행을 더 잘 하는 경향을 보였다. 상전두 영역은 배측 주의 신경망 (dorsal attention network)의 일부라는 점에서, 단서로 인한 하향식(top-down) 주의 처리와 섬피질의 부호화 기능과의 상호작용이 기억 과제 수행에 영향을 준 것이라 할 수 있다.

본 연구는 기억 조절과 관련된 신경 상관물을 알아보기 위하여 선행 연구에서 관찰된 후측 영역 내의 교차 주파수 관계를 먼 거리 영역 간의 관계를 포함한 대규모 신경망으로 확장하여 조사하였다. 그 방법으로 양분 그래프 필트레이션을 뇌자도를 이용한 뇌 신경망 분석에 처음으로 적용하여 다른 시간과 주파수 대역 간의

관계를 알아 볼 수 있었다. 뇌의 인지 과정이 특정 시간과 주파수 대역의 관계뿐만 아니라, 시공간 및 주파수의 다차원에서 상호작용하며 이루어지는 것이라 할 때 본 연구는 이러한 다차원적 뇌 신경망 연구를 향한 첫 걸음이 될 것이다.

주요어: 기능적 뇌 신경망, 알파 오실레이션, 감마 오실레이션, 뇌자도, 기억, 주의, 그래프 필트레이션

학번 : 2012-30033